Master of Science Thesis
MSFT02
VT2026

Investigation of a portable OSL reader for dosimetry applications during radiological or nuclear emergencies using ordinary salt (NaCl)

Tuva Borg Djurberg

Supervisors
Maria Karampiperi and Christian Bernhardsson

This work has been conducted at
Medical Radiation Physics, Skåne University Hospital, Malmö

Department of Medical Radiation Physics
Faculty of Science
Lund University, Sweden
www.msf.lu.se

Declaration of Use of Generative Artificial Intelligence

Grammarly, which uses generative artificial intelligence (GAI), was utilised to correct the spelling and grammar, as well as the tone and word choices, of pre-written texts.

Populärvetenskaplig sammanfattning

Vi lever i en tid av osäkerhet, med ett alltmer våldsamt globalt klimat. En vanlig rädsla är därför att en naturkatastrof eller konflikt kommer att leda till utsläpp av radioaktiva ämnen i miljön. Strålning är osynlig och något vi inte kan röra eller känna lukten av. Därför kan vi inte själva känna om vi har blivit exponerade för strålning innan det är för sent och allvarliga symptom redan uppkommit. Det är alltså inte konstigt att känslor av ångest är förknippade med tanken på att radioaktivitet sprids ut i naturen!

Osäkerheten om huruvida en exponering har inträffat är mångas största orosmoment. Ett sätt att övervinna detta är att etablera en metod för individuell övervakning. De kommersiellt tillgängliga mätarna, så kallade dosimetrar, är dock dyra, svåra att använda i en nödsituation och kan kräva lång transport för att nå en utläsningsstation. Men hoppet är inte ute. I våra hem finns ett billigt material som, när det förvaras i mörker, passivt samlar in information om omgivande strålning genom att lagra energi. Salt. Genom att sedan belysa saltet i en läsare med en metod som kallas optiskt stimulerad luminescens (OSL), får vi en signal som är proportionell mot exponeringen. Bygger vi dessutom upp ett nätverk av bärbara OSL-läsare, övervinner vi också utläsningsproblemet. Men en idé för en potentiell lösning räcker inte; dess genomförbarhet måste testas i praktiken. Detta arbete var ett första steg i denna process, där utläsning av salt med den bärbara OSL-läsaren Helios testades.

Tester utfördes i syfte att utveckla en metod för avläsning av signal från både vanligt salt från skafferiet och salt komprimerat till pellets. Eftersom informationen i saltet kan frigöras genom att belysa det med vilket ljus som helst, undersöktes även vanliga ljuskällor som mobiltelefoner. Att glömma att stänga av mobiltelefonen kan hända oss alla, men i detta sammanhang fruktades att en blinkande avisering skulle radera någon annans kvitto på huruvida de exponerats för farliga mängder strålning. Det visade sig dock att en påslagen mobil med ljusstyrkan på max kunde lämnas bredvid ett prov i flera minuter utan att saltet tömdes på information.

Vid en olycka vill vi få så exakt information som möjligt över ett brett spektrum av potentiell exponering. Mätningar gjordes därför både vid låga nivåer i samma storleksordning som en röntgenbildtagning och vid höga nivåer liknande de vid cancerbehandlingar. Anmärkningsvärt nog kan vi, genom att multiplicera signalen från saltet med ett enda omvandlingsvärde, koppla signalen direkt till storleken på en exponering i princip över hela det undersökta intervallet. Ytterligare undersökningar genomfördes för att fastställa hur låga exponeringar vi faktiskt kan mäta med hjälp av det utvecklade omvandlingsvärdet. Resultatet blev att vi med Helios-läsaren kunde mäta exponering ner till den naturliga nivån av strålning som härstammar från rymden och berggrunden.

Omedelbart efter bestrålning tömdes mycket av den energi som tillförts saltet av strålningen, trotts att saltet inte belystes. Signalen som avläste från ett saltpaket en timme efter exponering skiljde sig från den som mättes fyra timmar efter exponering, trots att alla korn i paketet exponerats för samma mängd strålning. Vid första anblicken verkar detta fenomen vara ett oöverstigligt hinder mellan oss och vårt mål att tillförlitligt mäta storleken på en exponering. Men redan en dag efter bestrålningen började signalen från saltet stabiliseras. För utvalda inställningar spelade det ingen roll om saltet mättes en vecka efter bestrålningen eller en hel månad senare; signalen som utlästes var densamma.

Saltmätningar med en bärbar avläsare visar stor potential för exponeringsövervakning. Processen är förlåtande om någon råkar tabba sig vid avläsning, kan ge korrekt information över ett stort intervall av strålningsnivåer, och om köer uppstår vid avläsning finns det inget att oroa sig för, eftersom signalen är mycket stabil under en lång tidsperiod. Det finns därför en god chans att vi, i händelse av en nödsituation, inte behöver leva i rädsla för en möjlig men obekräftad exponering. Det vill säga, så länge vi alla ser till att det finns salt hemma i skafferiet!

Abstract

In the event of a radiological or nuclear (R/N) emergency, individuals and/or population groups may be exposed to radiation. For the average civilian, a potential but not confirmed exposure causes anxiety, even though it is unlikely that anyone except first responders or those close to the emergency site receives doses above negligible levels. Thus, there needs to be a way to separate the unexposed but worried masses from those in need of immediate care, as well as means to conduct long-term population monitoring for epidemiological purposes. Preferably, such a method should be rapidly deployable.

A possible way to survey the population would be to distribute NaCl samples, which are easily mass-produced, and to set up a network of relatively inexpensive, portable optically stimulated luminescence (OSL) readers. The feasibility of this approach requires readers to be benchmarked for this purpose beforehand. This work investigates the portable reader Helios, which features two reader holders (flat and conical) and three LED options for the continuous-wave mode (blue light, IR light, and a combination of the two), in order to ascertain suitable readout protocols and characterise luminescent properties. Readout parameters for the Helios reader were determined for salt pellets and salt grains, based on their OSL/IRSL dosimetric properties. The potential effect of various laboratory conditions was also studied, including the standard procedure to expose samples to red light and emulating mishaps by exposing them to other light sources. During irradiation, only one side of a pellet will be facing the radiation source. This side of the pellet is not necessarily the side later facing the photomultiplier tube (PMT) and LEDs during readout. Whether or not the side of the pellet being read out coincided with the side of the pellet facing the source during irradiation had a significant impact on the intensity of the luminescence signal, according to a Mann-Whitney U-test. The difference in luminescence signal intensity was not considered large enough to affect triage during R/N emergencies. However, for research requiring more precise dose estimation, the dependence on irradiation geometry and readout orientation may have a greater impact.

For pellets, the reader showed a linear response over the dose interval 10 mGy-15 Gy for IRSL, while for blue light (OSL) and the combination of IR and blue, linearity was observed up to 7 Gy, after which the PMT was saturated. An overresponse at high doses was found for all readout geometries except OSL with pellets. When reconstructing doses using the sensitivity from the dose response curves, pellets read out for OSL yielded the most consistent results, with values never more than 10 % away from the theoretical dose. Minimum measurable dose (MMD) was 1.5 mGy for IR, 210 µGy for blue light, and 190 µGy for the combination. After irradiation, the signal stabilised within a matter of days for IR, indicating that correction for fading may not be necessary for readouts conducted more than 1 day after irradiation. Readout using OSL showed an inverse fading effect for at least 50 days after irradiation, suggesting that fading correction is necessary when the time between irradiation and readout is prolonged. A relatively linear dose response was observed for grains over the dose interval 50 mGy-5 Gy for both IRSL and OSL, but overresponse at high doses was present. For grains, dose reconstruction from IRSL measurements was superior, although the MMD was relatively high, 20 mGy. The MMD for OSL was 0.5 mGy. Inverse fading was observed, continuing for the first week after irradiation, after which the signal stabilised for IRSL but continued to increase for at least 15 days for OSL.

Based on these results, the use of the portable reader Helios, combined with NaCl samples, for dose monitoring during emergencies seems promising. Salt in pellet form greatly simplified the workflow compared with grains, but both are feasible options for monitoring due to their easy availability and favourable luminescent properties. OSL was superior for dose reconstruction with pellets and measurements of low doses. Its main disadvantage was persistent inverse fading, which could make the readout of samples stored for a long time more difficult. For grains, IRSL readout was preferable to OSL for dose reconstruction, but not at low doses. Still, more research is needed before a universal readout protocol can be devised, especially regarding the impact of environmental factors on the samples.

Contents

1 Introduction **5**

2 Background **5**
2.1 Emergency Preparedness and Response . . . 5
2.2 Optically Stimulated Luminescence . . . 6
2.3 Dosimetry . . . 7
2.4 Luminescent Properties . . . 8
2.4.1 Dose and Energy Response . . . 8
2.4.2 Signal Components . . . 8
2.4.3 Sensitivity . . . 9
2.4.4 Detection Limits . . . 9
2.4.5 Fading . . . 9

3 Materials and Method **10**
3.1 NaCl . . . 10
3.1.1 Pellets . . . 10
3.1.2 Grains . . . 10
3.2 Readout Units . . . 11
3.2.1 Helios . . . 11
3.2.2 Risø . . . 12
3.3 Irradiation . . . 12
3.4 Readout Protocols . . . 12
3.5 Signal and Error Calculation . . . 13
3.6 Measurements . . . 14
3.6.1 Readout Geometry . . . 14
3.6.2 Operating Current . . . 14
3.6.3 Number of Pellets Per Sample . . . 14
3.6.4 Mass for Measurements of Grains . . . 15
3.6.5 Dose Response and Detection Limits . . . 15
3.6.6 Dose Recovery Test . . . 16
3.6.7 Fading . . . 16
3.6.8 Pellet Orientation During Irradiation and Readout . . . 16
3.6.9 Accidental Light Exposure . . . 16

4 Results and Discussion **17**
4.1 Readout Geometry . . . 17
4.2 Operating Current . . . 18
4.3 Number of Pellets Per Sample . . . 19
4.4 Mass for Measurements of Grains . . . 21
4.5 Dose Response and Detection Limits . . . 22
4.6 Dose Recovery Test . . . 28
4.7 Fading . . . 30
4.8 Pellet Orientation During Irradiation and Readout . . . 31
4.9 Accidental Light Exposure . . . 32
4.10 Limitations . . . 34

5 Conclusion **35**

A Appendix **39**
A.1 Lightproof Holders . . . 39
A.2 Dose Response (OSL/IRSL Decay Curves) . . . 40

1 Introduction

In the event of a natural disaster or conflict that causes the release of radioactive substances into nature, plans to address this in a manner that minimises harm to citizens and the environment are required. Dose monitoring is an integral part of the radiological or nuclear (R/N) emergency response, both in the immediate aftermath and the years following. In the short term, accurately determining doses enables efficient triage and may help lessen anxiety amongst civilians, while in the long term, it facilitates epidemiological studies.

It has been proposed that salt may be utilised for dose monitoring in the event of an R/N emergency, with decentralised measurements carried out as needed using a network of portable OSL readers. An initial investigation of the feasibility of the above proposal using the portable OSL reader Helios will be conducted in this work. The aim is to develop a universal readout protocol for Helios by studying the luminescent properties of salt and the effects of environmental factors on salt samples during storage and readout.

2 Background

2.1 Emergency Preparedness and Response

During an R/N emergency, such as the failure of a power plant or the detonation of a nuclear weapon, both the surroundings in close proximity and areas farther away will be affected, according to a report by the Swedish Radiation Safety Authority (2023)[1]. The widespread distribution will occur due to large amounts of radioactive substances being released and mixed into clouds rising from the emergency site. These substances will then form smaller particles as the clouds cool, which may be further distributed over large areas by the wind [1]. In the event of an R/N emergency, action must be taken promptly to minimise harm to both citizens and the environment. A way to ensure this is to already have an established international framework that ensures both equipment, procedures and qualified personnel are available and ready to respond. Establishing, and later maintaining and expanding, a system to address R/N incidents is known as emergency preparedness and response (EPR). The IAEA has developed recommendations and guidelines for a functioning EPR[2].

The publication *Generic Procedures for Medical Response During a Nuclear or Radiological Emergency* in the EPR series (2024) details the response of hospitals during R/N emergencies[3]. A core part of this response is that hospitals need a way to assess and conduct effective medical triage for those affected by radiation. However, most acute symptoms caused by exposure to ionising radiation have a latency period that stretches from days to weeks, meaning that exposed individuals can be difficult to diagnose, either because the symptoms have yet to manifest or because medical personnel may struggle to connect symptoms to acute radiation syndrome (ARS). Thus, it would be beneficial to have a method allowing personnel to assess those suspected of having been exposed to radiation and the corresponding magnitude of the individual exposure[3]. It would also be advantageous when reassuring the "worried well", referring to individuals who seek hospital care during R/N emergencies due to understandable worry that they have been exposed, yet are either unexposed or exposed to radiation levels so low that no deterministic effects are expected and the risk of stochastic effects is small. One method for streamlining the triaging of externally exposed persons would be a mass screening using individual dosemeters[4]. However, at the moment, individually screening all citizens is not part of the emergency planning, due to a lack of enough dosemeters to cover an affected population and a way to deliver them, even if they had been available, according to Chumak et al. (2024). There are ways to estimate population doses retrospectively, but these methods require large-scale environmental measurements and modelling and are not very accurate on an individual level when radiation doses to many persons are to be assessed. Such calculations, while of value for the long-term monitoring, are difficult to perform in a useful time frame during the initial phase of the emergency[5]. The inhomogeneity of radioactive distribution and a probable lack of data from the initial time of the emergency also mean that these approximations vary by orders of magnitude even across adjacent areas. Such variety is problematic when attempting to make dose assessments

at the individual level[6]. A material that has been suggested for retrospective dosimetry is salt, but there are difficulties in translating a dose to salt to a dose received by humans. Fortunately, when individuals carry a salt dosemeter on their person, the translation problem can be circumvented while retaining salt's good dosimetric properties[7]. Thus, salt dosemeters could be a good option for individual screening, as they are both cost-effective and easy to distribute[5]. It is also something most people already have in their homes, meaning it may be possible to obtain information close to the beginning of the event for many citizens. The use of salt dosemeters also provides a means to obtain detailed information for long-term monitoring, such as in epidemiological studies.

The readout units for the above-mentioned measurements are usually stationary due to their weight and expense, and are bound by strict regulations as they contain a radiation source[8]. Thus, the readers are mostly found at dedicated research facilities and hospitals. However, in recent years, relatively afordable portable readers have been developed. Using these readers, it could be possible to set up a network that can be shipped wherever they are needed, which would not necessarily be hospitals. Having multiple portable readers could thus reduce strain on the healthcare system during R/N emergencies while at the same time swiftly providing the public with dose information.

2.2 Optically Stimulated Luminescence

Common table salt, sodium chloride (NaCl), is a crystalline insulator, indicating that the material has two properties of interest for optically stimulated luminescence as explained by Yukihara and McKeever (2011)[9]. The first property is due to its status as an insulator, meaning that the energy gap between the filled valence band and the conduction band is large enough that electrons cannot be thermally excited at room temperature. As a result, NaCl remains in a stable state when stored at room temperature. However, ionising radiation of sufficient energy can overcome the bandgap and electron-hole pairs may be created. The second property concerns the atomic structure of an alkali halide crystal, such as NaCl. These materials contain several defects, for instance missing or additional atoms in the lattice, known as vacancies and interstitials, respectively. The defects introduce additional energy levels within the bandgap[9]. These energy levels can either capture single charge carriers, known as either electron or hole traps, depending on whether the charge is negative or positive, or capture both positive and negative charge carriers, known as recombination centres according to Waldner (2021), see Fig. 1[10]. When excitation by ionising radiation occurs, charge carriers are created, with holes remaining in the valence band and electrons excited to the conduction band. However, the presence of the additional energy levels means that during deexcitation, some of the charge carriers get trapped instead of recombining in the valence band as they would if no defects were present[10]. If the potential difference between the trap and the conduction band is larger than what can be traversed by thermal energy, the probability that the charged particle escapes at room temperature is negligible. Given that energy sufficient to cross the potential difference is not introduced, electrons and holes are stored in the lattice near indefinitely. This is known as a metastable state[9].

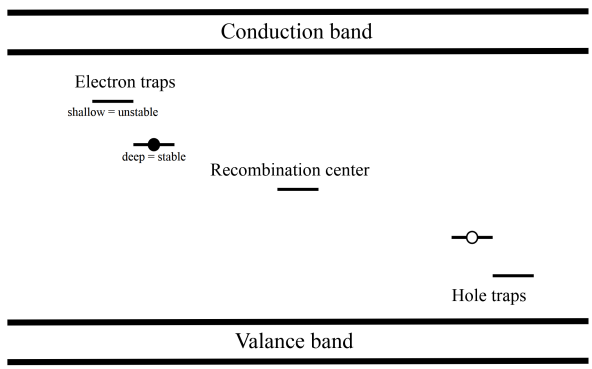

Figure 1: Energy band diagram of an insulator, with the energy gap between the valance- and conduction band, including additional energy levels created by defects in the material. These additional energy levels are known as electron traps, hole traps, and recombination centres.

As previously touched upon, an insulator remains in a metastable state unless receiving a sufficient amount of energy to re-excite the trapped electrons, so that they may once again travel to the conduction band. This additional energy can, for example, be imparted by bringing the sample into contact with light or heat.[10]. When the captured electron-hole pairs recombine in the crystal defects, photons in the visible spectrum will be emitted. If the means of transferring energy to the

crystal is light, this process is called optically stimulated luminescence (OSL). A detection device, such as a photomultiplier tube (PMT), is then used to detect the light emitted by the salt. The emitted light has a higher energy than that of the light used to stimulate the salt, which corresponds to the wavelength of the luminescence being shorter than that of the stimulating light ($E_{\text{emission}} > E_{\text{stimulation}} \implies \lambda_{\text{emission}} < \lambda_{\text{stimulation}}$). Note that the energy of the emitted photon originates from both the stimulation photon and the first excitation induced by ionising radiation, which is what allows the energy of the emitted photon to be higher than that of the stimulating photon. This phenomenon is utilised when discriminating incoming light in OSL. Optical filters that remove the stimulating light can be employed without affecting the luminescence detection overly much, as it is improbable that emission of light with a lower wavelength than that of the stimulation light from luminescence occurs due to "non-radiation-induced processes" according to Yukihara and McKeever (2011)[9].

The most commonly used stimulation light sources are green, blue, or infrared (IR) light-emitting diodes (LEDs)[9]. The light sources used to stimulate the salt operate in different modes; the most common are continuous wave (CW), linearly modulated (LM), and pulsed (P) as described by Thomsen (2004)[11]. This work focuses on CW-OSL, where stimulation is performed with light of a fixed intensity. In most cases, counts are recorded from the moment the light source is turned on, meaning that stimulation of the sample with light and detection of the resulting luminescence occur simultaneously. The method yields a high-intensity peak at the moment the light source is turned on, which then steadily decreases as the traps are depleted. Note that total depletion is usually not achieved. The resulting curve is called an OSL-decay curve, see Fig. 2[11]. If the intensity of the stimulation light is constant, then for an ideal OSL reader the integration of the decay curve will be proportional to the dose absorbed by the sample[9].

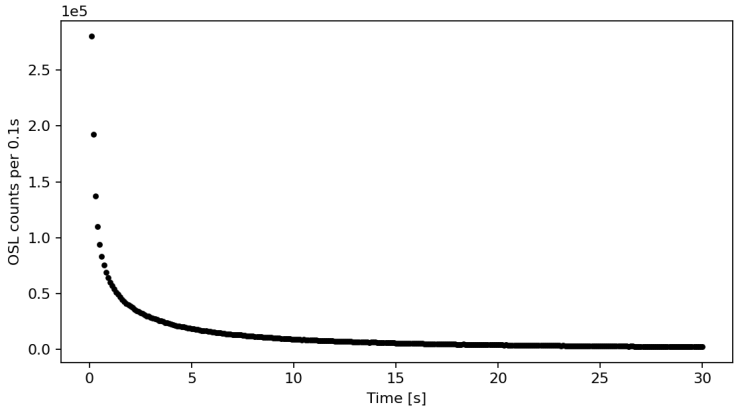

Figure 2: An OSL-decay curve of salt pellets irradiated with 1 Gy, showing OSL counts per 0.1 s as a function of stimulation time.

2.3 Dosimetry

Retrospective dosimetry is a common application of OSL, in which the OSL signal is related to the dose absorbed by the material after irradiation. The method can be applied to estimate exposure during or after R/N emergencies, which is what this work will focus on[11].

Dosimetry during R/N emergencies can be further divided into whether it investigates the early stages of an accident for triage or concentrates on long-term monitoring in the aftermath according to Bailiff, Sholom, and McKeever (2016)[12]. The focus during early stages is on deterministic effects, largely caused by external exposure, and is monitored over a shorter timeframe. As discussed earlier, such monitoring is most beneficial when done at an individual level. For triage purposes, the doses of interest are between 0.5 Gy and 10 Gy, with the most critical dose being around 2 Gy. Triage personnel are encouraged to send people home if they have been exposed to doses below 1 Gy, as the risk of developing ARS symptoms below this threshold is low. It is thereafter recommended to keep people who have been exposed to between 1 Gy and 2 Gy under observation or schedule them

for follow-up appointments at a later date, as they may develop mild ARS symptoms. Mortality risk has been observed to increase above the 2 Gy threshold, becoming progressively more severe as exposure dose grows. Individuals exposed to doses above 2 Gy should therefore be offered immediate hospital care. If OSL is used for triage during an R/N emergency, the materials used must therefore properly reflect the radiation exposure from the event[12]. The people who may receive high enough doses to result in ARS symptoms are either those present at the start of the R/N emergency or first responders. It is unlikely that the surrounding population who are either evacuated or live in a contaminated area further away from the initial site receives doses above the 2 Gy threshold[13]. Triage allows hospitals to prioritise those that need healtcare the most, lessening the burden on the system during R/N emergencies. Moreover, monitoring both individual and population exposure among those receiving low doses remains useful for studies of stochastic effects and epidemiology as well as to provide information to the public[12].

2.4 Luminescent Properties

2.4.1 Dose and Energy Response

The relationship between the dose a sample receives during irradiation and the read out OSL signal is referred to as the dose response. When used for retrospective dosimetry, it is preferable if the dose response is linear, and it must be reproducible[10]. To accurately determine the dose from the signal output, the dose range over which the linear response is observable must be determined.

Another parameter of interest for each material intended for OSL dosimetry is the energy response, that is, the relation between the energy of the ionising radiation and the OSL signal. A theoretically optimal OSL dosemeter has the same energy response as tissue, which requires that the effective atomic number Z_{eff} is close to that of soft tissue and water ($Z_{\text{tissue}} = 7.65$ and $Z_{\text{water}} = 7.51$, respectively). The benefit of tissue equivalent materials is that the readout signal can be directly compared to the absorbed dose a person has received. However, the effective atomic number of NaCl is double that of water ($Z_{\text{salt}} = 15.2$)[14]. That difference in Z_{eff} becomes of importance at lower energies where the photoelectric effect dominates, as a higher atomic number results in a noticeable over-response in this region due to the $Z^{3\text{-}4}$ dependency. However, dosemeter holders with special filters can be utilised to smooth out the energy response [15].

2.4.2 Signal Components

When estimating the dose received by a population or an individual during R/N emergencies, two components must be considered when evaluating the OSL signal, according to Thomsen (2004)[11]. The first component is caused by excitation from the natural background, such as cosmic radiation or naturally occurring radioactive material (NORM). Information about the natural background dose goes back to the last zeroing event that emptied all OSL traps, which, for salt, is either heating during manufacture or exposure to direct sunlight. When distributed as dosemeters, the last light exposure will be the zeroing event, after which the natural background accumulates during the period the dosemeter is worn. This contribution is likely negligible in relation to other radiation sources during an R/N emergency. The second component is caused by possible radiation exposure during the radiological emergency, known as the transient dose, and is layered on top of the natural background. For dosimetry purposes, what is of interest is the transient dose. For the best approximation of the transient dose, the background should be subtracted from the measured OSL signal[11].

There is a contribution to the OSL signal from photomultiplier tube (PMT) dark counts, filter breakthrough, and very deep traps with low sensitivity to stimulation light that empty slowly. The first two components should always be corrected for and are collectively referred to as the inherent background signal, while the latter component is of most importance for repeated irradiation and readout of the same sample[11].

2.4.3 Sensitivity

The sensitivity of a material is defined as the emitted luminescence per unit dose[11]. This property can be determined using the dose response curve, specifically the gradient from a linear function through the origin ($y = kx$, where the sensitivity is k)[4]. For this work, it means that

$$\text{signal} = \text{sensitivity} \cdot \text{dose}. \tag{1}$$

The material may be measured using different geometries and in varying amounts, from which it follows that the mass does not remain constant. For comparison purposes, the signal can thus be normalised to mass, such that

$$\text{signal/mass} = \text{sensitivity} \cdot \text{dose}. \tag{2}$$

2.4.4 Detection Limits

Even in an R/N emergencies, most of the population will not be exposed to doses higher than those from the normal background. Thus, the ability to accurately characterise samples exposed to only a few mGy or µGy is of interest, but to do so, the lower readout limits must be known. There are two types of readout limits: minimum detectable dose (MDD) and minimum measurable dose (MMD). Both limits depend on how large the background signal of the reader is. The more background signal there is, the harder it is to distinguish the natural signal fluctuations from the few emitted photons that result from a low-dose irradiation[10]. The MDD is calculated as ten standard deviations from measurements of blank pellets (σ_{blank}), where the signal is converted to dose using a dose response curve (Eq. 3). The MMD can be calculated the same way as MDD, only using three standard deviations instead of ten[16]. That is,

$$\text{MMD} = \frac{10 \cdot \sigma_{\text{blank}}}{k} \quad \text{and} \quad \text{MDD} = \frac{3 \cdot \sigma_{\text{blank}}}{k}, \tag{3}$$

where k is the sensitivity.

There is also an upper limit of what can be measured. For some materials, this limit occurs when samples are exposed to very large doses, such that nearly all traps are filled. This is known as saturation of the material. For other materials, the measurement limit occurs not due to sample properties but because the luminescence is large enough to saturate the PMT. For both these cases, the dose-response curve ceases to be linear. Instead, the relationship between signal and dose becomes sublinear, where the ratio between the two decreases as the dose increases[10].

2.4.5 Fading

The phenomenon known as fading refers to both short- and long-term loss of the OSL signal according to Yukihara and McKeever (2011)[9]. The short-term loss of the OSL signal is seen in measurements performed too close in time to the irradiation with ionising radiation. This loss of signal is due to an initial depletion of shallow traps from thermal energy, which occurs over a time frame of minutes to several hours, depending on the material. Readouts performed before this initial fading will include contributions from the shallow traps, and thus a measurement performed immediately after irradiation will exhibit a relatively high signal intensity. As the pause between irradiation and readout increases, measurements will show a gradual decrease in intensity until the metastable state is reached. After passing that point the intensity of the signal remains constant[9]. Quantum tunnelling is also a source of fading, specifically anomalous fading. Charges located in deep traps that are stable at room temperature may, due to tunnelling effects, reach proximately located recombination centres and release luminescence. The tunnelling probability decreases with added distance between traps and recombination centres, in effect meaning that after an initial fast depletion of neighbouring charges and centres, the rate of recombination as a result of tunnelling decreases[17].

To ensure a reliable relationship between the OSL signal and the dose received measurements cannot be performed until the rapid fading has passed. Thus, a waiting period is required between irradiation and OSL measurements. If a shorter time between irradiation and OSL readout is desired, an alternative to waiting for the shallow traps to naturally empty is to preheat the samples[10]. For retrospective dosimetry, initial rapid fading is generally not a problem, as readouts are not conducted too close in time to the exposure event. However, fading on a longer timescale could be an issue. For an ideal dosemeter material, the charge leakage over a long period should be negligible. In reality, the signal intensity still exhibits a minor decrease over time. How much depends on the material[9]. For irradiated NaCl, most studies indicate that the signal is stable over time after the initial rapid fading, although some studies show a tendency toward inverse fading if a long time period elapses. That means, if the salt is stored for a long period before readout, the signal intensity increases again[4].

3 Materials and Method

3.1 NaCl

3.1.1 Pellets

Two 1000 g packages of common Swedish household mine salt (Falksalt, "finkornigt salt"), consisting of 99.9 % NaCl with added iodine (5 mg/100 g) and anti-caking agents E535 and E536, were used in the production of two batches of NaCl pellets[18]. The salt was sieved before pellet production such that only grains between 100 µm and 400 µm remained, as this grain size range was shown to produce the most mechanically stable pellets in a previous study [16]. The pellets were then manufactured using a manually operated tablet press (TDP 0 Desktop Tablet Press, LFA Machines Oxford, Ltd). All pellets had a diameter of 4 mm, but, given that the pellets were produced in different batches, during which the press settings were changed due to other work, the exact thickness (and consequently mass) settings varied slightly between batches. The pressing process introduced an additional spread in thickness and mass within a batch, with standard deviations of approximately 0.1 mm for thickness and 1 mg for mass (Tab. 1).

Table 1: The mean and standard deviation of the pellets width, thickness, and mass for two different production batches. The standard deviation is given as the uncertainty. Both the width and thickness was measured with a caliper with an measurement error of ±0.2 mm, while the scale used to weight the pellets had a measurement error of ±0.1 mg .

Batch	**width** [mm]	**thickness** [mm]	**mass** [mg]
1	4.007 ± 0.005	0.92 ± 0.04	24 ± 1
2	4.003 ± 0.005	0.86 ± 0.05	22 ± 1

Before any of the pellets were irradiated, they were allowed to rest for at least 3 days, in accordance with previous research by Waldner, Rääf, and Berhardsson (2020)[19]. The storage period is necessary when using NaCl pellets because the readout signal for a constant dose decreases with the time between production and initial irradiation during the first three weeks. The effect is most notable the first two days after production. Nevertheless, as long as the NaCl pellets are not used to investigate long-term radiation exposure, a storage period of three weeks before irradiation is not needed to reach a more stable signal, given that the initial two-day rapid drop in signal sensitivity has passed[19]. Before irradiation, the pellets were stored in a transparent container and exposed to a mixture of natural and artificial light until irradiation to avoid storage of signal from the natural background.

3.1.2 Grains

Salt sachets produced in Spain containing grains were also irradiated. Each sachet contained 1 g of salt[20]. The grains were stored in a mixture of natural and artificial light in the same location as

the pellets before irradiation. Grains were not sieved before readout and were scooped directly from the sachets into the respective readout holders, whereupon mass of the sample was determined.

3.2 Readout Units

Two readout units were used in this work, one portable (Helios) and one stationary (Risø), each with several different settings. Details on the filter brands, light sources, and PMTs for each reader are provided in Tab. 2.

Table 2: Reader-specific information about filter brands, light sources and PMT from [21] for Helios and from [8] and [22] for Risø.

	Helios	**Risø**
Detection filters	NIR Blocker Schott UG11 dielectric coated (2 mm thick) UG1 (3 + 3 mm)	Hoya U-340 (5 mm and 2 mm thick)
LEDs	LED1 (blue light, λ =470 nm) LED2 (IR light, λ =850 nm)	Blue LEDs (blue light, λ =470 nm) IR LEDs (IR light, λ =850 nm)
PMT	H11870-02-Y005 (Hamamatsu) Spectral range 300-650 nm	ElectronTube PDM9107-AP-TTL-06 Spectral range 280-630 nm

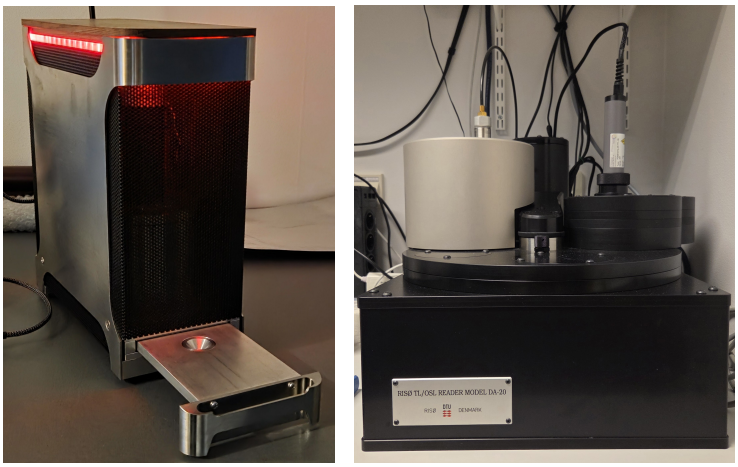

(a) (b)

Figure 3: The readers (a) Helios and (b) Risø.

3.2.1 Helios

The Zero-Rad Helios unit is a portable OSL reader (Fig. 3a) with two readout holders, one conical and one flat. Stimulation with both blue (LED1) and IR (LED2) light is available, with the LEDs usable separately or simultaneously (LED12). The LED intensity is regulated by the current (I). For LED1, the upper threshold of current is 90 mA, and for LED2, the maximum is 300 mA. It is not recommended to use the detector at more than 80 percent of the maximum curent. Should the photomultiplier range be exceeded, it displays a message indicating that the PMT is blind. This means that if the PMT is saturated, it can be noted during measurements. The reader has a mass of 4.8 kg[21]. In this work, the Helios reader was operated in CW spectrum mode, which performs regular CW-OSL, requiring the number of data points ("*samples*") and the *sampling period* as inputs. At the same time, the collection time is automatically calculated as the product of the two inputs.

3.2.2 Risø

The Risø reader (DA-20) is a stationary research thermoluminescence (TL) and OSL reader with a weight of about 80-90 kg (Fig. 3b). A sample can be placed in a shallow stainless-steel cup, which can then be placed in a sample carousel that holds up to 48 cups at once. Readout is performed one sample at a time at the measurement position, where a cup is lifted closer to the PMT and stimulated with blue or IR LEDs[8]. The optical power can be set from 1-100 %, where 40 % (34.4 mW cm^{-2} for blue light and 139 mW cm^{-2} for IR light) was used throughout this work, in combination with filters[23]. Note that OSL and IRSL cannot be used simultaneously with this reader, as this is not standard practise. The CW-OSL mode was used for the readouts in this work[8]. In Risø, the required input was the duration of a measurement ("time"), and how many data points should be recoded during stimulation. Optionally, data points could be collected while the stimulation light was turned off at the beginning and end of the measurement. The total number of data points and the time in seconds data was collected for each data point ("time per data point") were automatically calculated from the input.

3.3 Irradiation

The Risø DA-20 reader includes a beta source (^{90}Sr/^{90}Y) with a dose-rate of 4.48(13) mGy s^{-1} at the time of irradiation, which was used to perform beta irradiations of samples in the carousel (Fig. 4a). However, as samples in the carousel are approximately 17 mm apart, irradiation of one sample results in neighbouring samples also being irradiated, a phenomenon known as irradiation crosstalk. Measurements by the supplier show that the irradiation crosstalk is 0.25 % for directly adjacent samples, and then lessens to 0.014 % for the following sample[8].

A radiotherapy unit located at Skåne University Hospital, Lund, containing a ^{60}Co source (4410 TBq in March 2014) was also utilised for gamma irradiations. Pellets were placed in a PMMA phantom with a capacity to hold up to 100 pellets at once when a grid was used (Fig. 4b). The grid holding the pellets could be removed, allowing the space to be used to irradiate other sample geometries. In this work, the space was used to irradiate grains in groups of either 6 or 9 sachets (Fig. 4c). In addition to the space holding samples, a 5 mm PMMA cover was placed between the samples and the radiation source to create a build-up. Thus, large amounts of either pellets or grains were irradiated simultaneously while receiving the same dose. Irradiation was performed at two calibrated distances where the dose rates were 0.5001(8) mGy s^{-1} ("far" position) and 8.243(2) mGy s^{-1} ("close" position) at the time of irradiation.

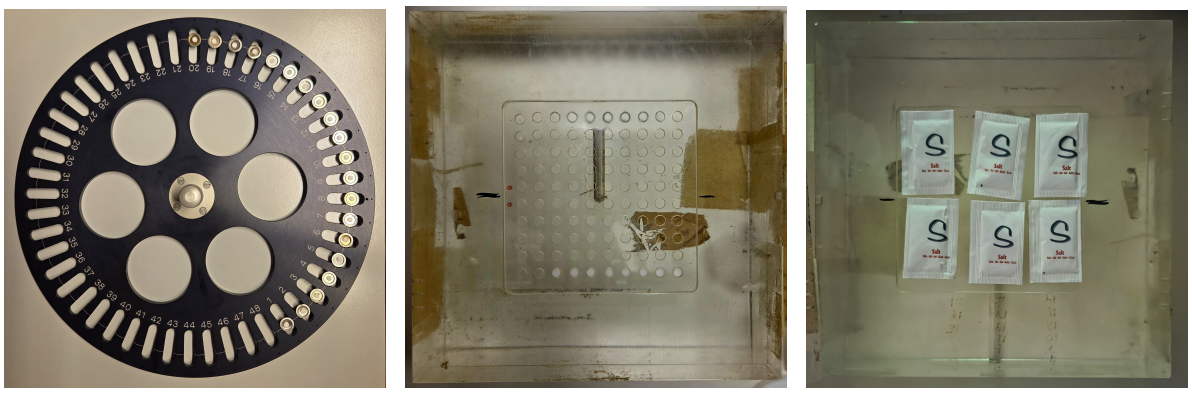

(a) (b) (c)

Figure 4: Samples to be irradiated placed either in (a) a Risø sample carousel, or in a PMMA phantom (b) with a grid or (c) without a grid. Samples irradiated using geometries seen in (a) and (b) were pellets, and in (c) grains.

3.4 Readout Protocols

During measurements with the Helios reader, the *CW Spectrum* mode was used, with number of recorded data points ("*samples*") set to 300 and *sampling period* set to 0.1 s, unless otherwise stated.

After a test to determine the optimal input current, 63 mA was used for LED1 and 210 mA for LED2 for subsequent measurements. If other currents were used, this is noted in the method description for that experiment. For the Risø reader, readouts were either 30 s or 60 s long, and always with a sampling period of 0.1 s. For both OSL and IRSL 40 % of the maximum power was used.

3.5 Signal and Error Calculation

The integral of the OSL-decay curves measured with Helios was approximated using the composite trapezoidal rule. For measurements done with the Risø reader, the integrals were instead calculated in Risø Analyst using the built-in integration function.

The background signal was determined by measuring unirradiated pellets and then integrating the initial part of the signal, using the same time interval used for the signal calculation of the irradiated pellets[4]. The entire OSL-decay curve was not used for dose estimation, as it has been shown that the smallest statistical uncertainty is achieved by integrating only the beginning of the OSL decay curve. This section includes emission light originating from the traps most sensitive to stimulation light. Further benefits of only using the initial part of the curve includes an "enhanced signal-to-noise ratio"[11].

After the integral over the readout time was decided for both irradiated and blank pellets, the arithmetic mean for irradiated and unirradiated pellets was calculated. The latter were used to subtract the background from the readouts of the irradiated pellets. Henceforth, the background-corrected mean is referred to as the signal. Note that after a dose response test was conducted, the integration time for pellets was primarily set to 1 s, but for certain measurements 15 s for blue LEDs and 30 s for IR LEDs was used for comparison purposes. For grains an integration time of 1 s, with 10 s sometimes also used for comparison purposes.

The variation between samples was of interest; thus, the standard deviation was used throughout this work to calculate uncertainties. Given that the data consist only of random samples, Bessel's correction was used to obtain a more unbiased estimate. That is, the standard deviations for blank and irradiated pellets were calculated using the divisor $(n-1)$, known as the sample standard deviation[24]. The sample standard deviation for the signal could then be calculated as

$$\sigma_{\text{signal}} = \sqrt{\sigma_{\text{irrad}}^2 + \sigma_{\text{blank}}^2}. \tag{4}$$

In the cases where the mass of the pellets or grains was measured, a signal normalised to mass was calculated. This was done by dividing the integrated OSL curve by the sample mass, for both irradiated and un-irradiated samples, and then subtracting the background normalised to mass. The signal error was then calculated using Eq. 4, where the sample standard deviation was calculated from the normalised integrals.

For some tests, it was also of interest to express the standard deviation as a percentage of the sample mean. This is known as the coefficient of variation (CV) and is calculated as

$$CV = \frac{\sigma_{\text{signal}}}{S}, \tag{5}$$

where S is the signal[25].

The data was fitted to a function using linear regression, either using a linear function $f(x) = kx$ for the linear scale or a power function

$$f(x) = ax^b \iff \ln f(x) = \ln a + b \ln x$$

for the logarithmic scale. For the logarithmic scale, the coefficient m was used to determine whether the data behaved in a linear ($b = 1$), supralinear ($b > 1$), or sublinear ($b < 1$) manner[26]. The coefficient of determination (R^2) was calculated for the models.

3.6 Measurements

3.6.1 Readout Geometry

Different readout geometries were investigated to determine how the signal varied with the holders used and the extent to which the signal could be improved by moving the samples closer to the PMT for the Helios reader. As samples which in part or entirely covered the reflective bottom of a holder were studied, the effect of not having a reflective area underneath the sample was also investigated. In total, five different readout geometries were studied. First, the conical holder (without modifications), and then four different setups for the flat holder; no modifications, a black paper placed at the bottom of the holder, a 3.8(2) mm thick piece of Styrofoam placed in the holder with a piece of black paper on top, and the same Styrofoam cutout but with a reflective piece of aluminium foil placed on top (Fig. 5). Five pellets were beta irradiated with 20 mGy for each setup, and read out 1 h after the last pellet was irradiated. For each geometry, five blank pellets were also measured. A current of 0.06 A was used for LED1 and 0.2 A for LED2 (67 % of maximum current for both).

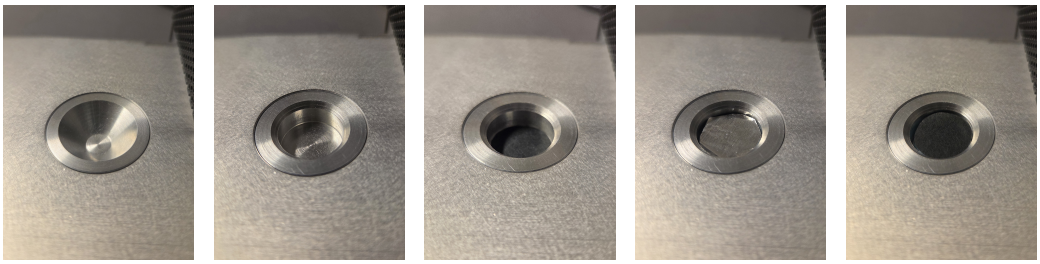

(a) (b) (c) (d) (e)

Figure 5: Five readout geometries where either (a) a conical holder, (b) a flat holder, (c) a flat holder and paper, (d) a flat holder and Styrofoam and aluminium foil, or (e) a flat holder and Styrofoam and paper were used.

3.6.2 Operating Current

To investigate if the current of the LEDs was stable and to find an optimal operating current, readouts using six different currents were conducted, were the data points were evenly spaced within an interval of 10-80 mA for LED1 and 50-250 mA for LED2. Pellets were beta irradiated with either 20 mGy or 90 mGy, whereafter a wait of 1.5 hours readout began: five blank pellets, five pellets which received dose 20 mGy, and five pellets which received 90 mGy for each input current. Each pellet was read out one at a time in the flat holder.

3.6.3 Number of Pellets Per Sample

Better statistics can be obtained by measuring multiple pellets simultaneously, while also achieving a higher signal. The effect of number of pellets per sample being read out was thus investigated using the flat holder. Using beta radiation, pellets were irradiated with a dose of 90 mGy, and after 1 h, readout began. Pellets were placed in groups of 1, 3, 5, 7, 9 pellets per sample (Fig. 6), and three readouts per group were conducted for each LED. This was done for both irradiated and blank pellets. The above method was then repeated for a dose of 20 mGy.

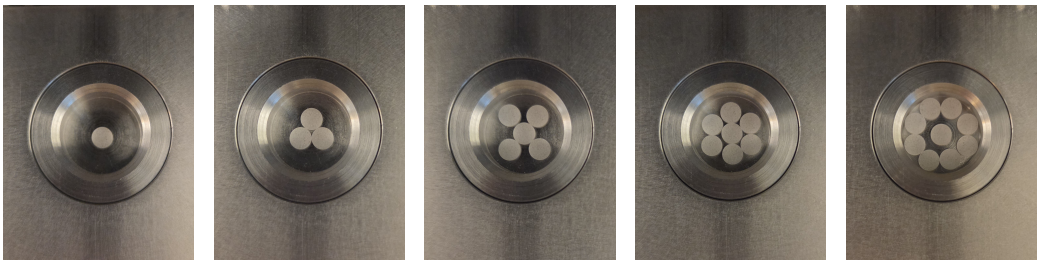

(a) (b) (c) (d) (e)

Figure 6: Placement of (a) 1, (b) 3, (c) 5, (d) 7, and (e) 9 pellets in the flat holder for Helios.

For samples irradiated with 20 mGy, the resulting signal was normalised to both the "specific weight" and the "mean weight". The specific weight was obtained by weighing the pellets after each measurement. In contrast, the mean weight was calculated by multiplying the number of pellets by the mass calculated after the pellet production for the batch used (the first batch) (Tab. 1).

3.6.4 Mass for Measurements of Grains

Before salt grains were measured in Helios, the effect the amount of salt used per sample had on the readout signal had to be determined. To do this, an initial concept test was conducted using the same salt used to make the first batch of pellets. The grains (unsieved) were scooped into a plastic bag and gamma irradiated with a dose of 500 mGy. After a 3 h wait, readout in Helios began. The flat holder was weighed using a scale, which was then zeroed at this mass. A small amount of salt was then scooped into the flat holder until its bottom was nearly covered by a single layer of grains, after which the holder, including salt, was weighed and the mass recorded. Three measurements were performed with the same amount of salt (± 5 mg), after which the amount of salt scooped into the holder was gradually increased. A total of eight masses were investigated for LED1 and six for LED2. To approximate the background signal, three measurements for the least, middle, and largest amounts of salt were conducted, and the average of all integrated OSL backgrounds was calculated.

This test was later repeated using salt grains in sachets. Nine sachets were gamma irradiated with a dose of 500 mGy. Note that the irradiation was done on two separate occasions for LED1 and LED2. The grains were then poured into the flat holder, and the mass was weighed using a scale. Readout began 1 d after irradiation, with measurements carried out for 50, 150, 300, 500, 100, 200, 400 mg (in this specific order), using four samples per mass, for statistical purposes. The maximum deviation of weight was 8 mg. The background was approximated using four measurements each for 50 mg and 500 mg, from which the average integrated OSL backgrounds was calculated.

3.6.5 Dose Response and Detection Limits

To create dose response curves and find detection limits, pellets were irradiated using the ^{60}Co source with 16 doses in the dose range 10 mGy-15 Gy for readout in the Helios reader and 13 doses in the range 10 mGy-5 Gy for readout in the Risø reader (Tab. 11). The samples were stored in dark conditions for approximately 1 d between the irradiations and the start of readouts. The readouts were conducted with six different setups, in which samples placed in the flat- or conical holder were read out with either LED1, LED2, or LED12. For the conical holder, one pellet was read out at a time, whereas for the flat holder, three pellets were used per sample. For each geometry, five readouts per dose (including blanks) were performed for statistical purposes. Because of the number of individual measurements, the readout was conducted over two days. The OSL/IRSL decay curves were used to determine a suitable integration time for each stimulation mode. Parallel to the Helios readout, five pellets for each dose were read out with the the Risø reader for OSL and IRSL (30 s). After the initial readout, the pellets were irradiated with a test dose of 45 mGy, which was read out after an additional hour. A dose response curve was then constructed for the Risø reader, both for the signal and test-dose-normalised signal.

Linear regression was applied to the dose response curves for both the Helios and Risø reader and used to calculate the MMD and MDD for the different stimulation modes and geometries. Additional blank measurements were performed to find the standard deviation, using 15 blank pellets for the Risø reader and the conical holder in the Helios reader, and 15 samples for the flat holder with 3 pellets per sample.

Similarly, a dose response curve for grains from the salt sachets was carried out for six doses in the range 50 mGy-5 Gy, irradiated at the ^{60}Co source (Tab. 11). Readout began 1 d after irradiation. Five samples of 20 ± 5 mg per dose were read out in the Risø reader, and five samples of 150 ± 10 mg per dose were read out in the Helios reader, for both blue- and IR LEDs. 15 blank measurements were taken and used to calculate MMD and MDD for grains.

3.6.6 Dose Recovery Test

To evaluate if the dose response curves could be used to estimate radiation exposure during an R/N emergency, a blind test was conducted. Pellets and grains were gamma irradiated at the close position at the ^{60}Co source for three different time durations. The irradiation times were unknown to the operator who read out the signals up until the point were doses had been calculated. Readout began after a 1 d storage period, for both OSL and IRSL. Five samples were read out per dose for statistical purposes, one pellet per sample in the Risø reader and three pellets per sample in the Helios reader. For grains, samples had the mass 20 ± 5 mGy in the Risø reader and 150 ± 5 mGy in the Helios reader. Using the relationship described in Eq. 1 and Eq. 2, the read out signals were converted to doses, referred to as reconstructed doses (D_{recon}). These were then compared with the theoretically calculated doses (D_{theo}), estimated by multiplying the dose rate by the irradiation times.

3.6.7 Fading

To characterise the fading of the pellets, pellets were irradiated with a dose of 500 mGy using the ^{60}Co source at the close position. Fading measurements were carried out from between 2 h and 50 d after irradiation. The signal from three pellets per sample was measured in the Helios reader using the flat holder, with five measurements taken per data point for LED1 and LED2. Five pellets per fading period were also read out in the Risø reader for both blue- and IR LEDs (60 s). Additionally, the pellets read out in the Risø reader were given a test dose of 250 mGy, and the signal was measured again after 1 h. The time elapsed between irradiation and measurement was calculated.

Fading was also investigated for the grains in sachets. In batches of six, twelve sachets of grains were irradiated at the ^{60}Co source at the close position, receiving to a dose of 500 mGy. After waiting from 1 to 15 d, the samples were read out in both the Helios and Risø reader using blue or IR LEDs, with five samples measured per data point. In the Helios reader, 150 ± 5 mg of grains was used per measurement, while for the Risø reader 20 ± 5 mg was used. The time elapsed between irradiation and measurement was calculated.

3.6.8 Pellet Orientation During Irradiation and Readout

When irradiating many pellets at once, it is usually most convenient to transfer the samples to small bags for transportation. However, using this transportation method, it is not possible to determine which side of the pellets faced the source during irradiation without marking the pellets. It was thus of interest to investigate whether the signal depends on which side of the pellet is read out in relation to its orientation during irradiation. Pellets were either beta- or gamma-irradiated, after which the pellets were maintained in their original positions with the irradiated side of sample facing up during transportation and storage (1 d). The pellets were then read out in the Risø reader using both OSL and IRSL. "Correct" side indicates that the side of the pellet that was read out coincided with the side which faced the source during irradiation, while "flipped" indicates that the pellet has been turned such that the side which faced away from the source now pointed towards the PMT.

3.6.9 Accidental Light Exposure

Pellets and grains are handled in red light to prevent premature emptying of the traps. It is thus of interest to investigate whether prolonged red-light exposure affects the stored energy. Additionally, even with care, accidental exposure to other light sources, such as a computer/mobile screen or a lamp, is likely to occur at some point due to human error. Another point of interest is thus to investigate by how much the signal decreases after accidental light exposure. To perform these tests, pellets were irradiated in 3D-printed lightproof holders, while grains were irradiated in lightproof mylar bags, all at 500 mGy (Fig. 7). Note that only four sachets would fit in the mylar bag at once, so irradiation was performed in two batches for grains.

(a) (b)

Figure 7: Two irradiation geometries for irradiation of (a) 3D-printed light-proof holders containing pellets and (b) a lightproof mylar bag containing four salt sachets.

To test the effect of red light, the salt was removed from the lightproof holders in the dark and then placed in holders on the Risø reader sample carousel underneath the red light source for 5, 10, 30, and 60 min. For each period, nine readouts were performed for both pellets and grains. The samples were read out using OSL and calibrated with a dose of 250 mGy. To test the effect of accidental exposure, the covering of the 3D-printed holder was removed, and the now opened holder was placed next to the device/underneath a florescent tube ceiling lamp for 5 min. The same was done for the grains. The sachets were removed from the mylar bag and placed next to a light source. Note that when the samples after this were placed in the carousel according to standard procedure, they were exposed to red light for 5 min for pellets and 10 min for the grains.

4 Results and Discussion

4.1 Readout Geometry

The highest signal for a holder without modification was obtained with the conical holder. Compared to the flat holder, the mean signal for the conical holder was 34 % higher for LED1 and 9 % higher for LED2 (Tab. 3).

When moving the sample closer to the PMT, the signal improved compared to the unmodified flat geometry, especially for LED2, where the signal more than doubled (Tab. 3). The increase for OSL was 15 % and for IRSL 122 %. However, having an extra non-attachable component will come with two major issues when using a network of portable readers in practise. First, replicating the same geometry for all readers using Styrofoam and a reflective material (or an equivalent 3D-printed component) will be difficult and adds unnecessary uncertainty. Second, having an extra piece to keep track of in an emergency might have negative consequences, because, unlike the holders, which can be securely attached to the reader and are easy to transport, the extra component must be carried separately. Requiring an extra component that may get lost as a necessary part for dose estimation is an added complication. Unless it is crucial to perform IRSL measurements, it is better to use holders as is without modification. Whether the conical holder or the flat holder without alterations is the most suitable measurement geometry will be further investigated in this work.

Excluding the case where the sample was moved closer to the PMT and a reflective bottom was used for LED2, the conical holder produced the highest signal across all readout geometries. However, the coefficient of variation (CV) was the smallest when using the flat holder without alterations. For the other geometries, the CV was above double that of the flat holder without modifications. If the reflective area underneath the sample was covered, the signal decreased while the CV increased, with the exception being between “Flat + S.F. + Al.” and “Flat + S.F. + Paper” for LED1 where CV was 1 percentage unit lower.

Table 3: The mean of five background corrected readouts (signal) for five different measurement geometries, where the mean signal have been normalised to the flat geometry. The coefficient of variation (CV) of the signal has also been calculated. Note that S.F. stands for Styrofoam and Al. stands for aluminium.

Geometry		**LED1**		**LED2**	
		Meas.	Norm.	Meas.	Norm.
Cone	Signal [counts]	940 ± 80	1.34	22 ± 3	1.09
	CV [%]	8	-	13	-
Flat	Signal [counts]	710 ± 20	1.00	20 ± 1	1.00
	CV [%]	3	-	5	-
Flat + Paper	Signal [counts]	400 ± 100	0.61	12 ± 2	0.58
	CV [%]	24	-	20	-
Flat + S.F. + Al.	Signal [counts]	800 ± 100	1.15	46 ± 5	2.22
	CV [%]	13	-	11	-
Flat + S.F. + Paper	Signal [counts]	540 ± 60	0.77	16 ± 2	0.78
	CV [%]	12	-	14	-

4.2 Operating Current

For LED1, the signal increased with input current. However, it exhibited more stable behaviour for input currents above 52 mA, as the intensity was high enough that most traps were emptied within the stimulation time (Fig. 9a). The same trend of stabilisation was not observed with LED2, because IR emptied the NaCl traps slower and never completely (Fig. 8b).

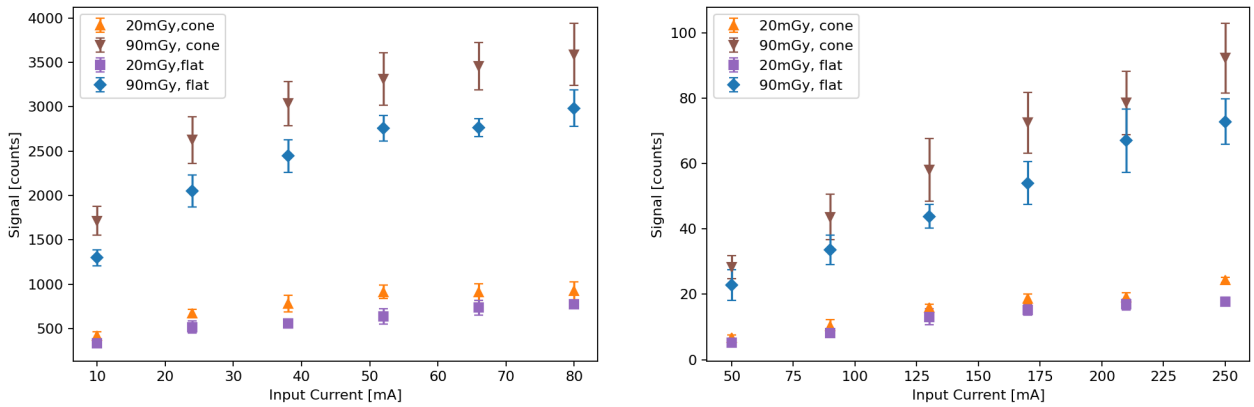

(a) (b)

Figure 8: Signal as a function of input current for pellets irradiated with 20 mGy or 90 mGy and read out with the Helios reader using (a) LED1 or (b) LED2.

The mean operational current was always lower than the input current, as shown in Fig. 9. For higher input current values, this discrepancy was reduced, with the mean operational current reaching 90 % of the input current by 66 mA for LED1, and reaching 98 % of the input current by 250 mA for LED2 (Tab. 4). However, in order to maintain long-term stability of the reader it is not recommended to operate the LEDs at more than 80 % of maximum current, so a lower input current than that is required.

For most inputs, the current in LED2 remained relatively stable, with a small standard deviation relative to the input current. LED1 showed higher instability, while the minimum and maximum currents during a measurement could be more than half or double that of the input current (Fig. 9). Notably for LED1, up to at least 52 mA the lowest current value during a stimulation was always 0 A, and at input current 10 mA the mean operational current was near 0 A. It was reasoned that using 70 % of the maximum current was the most suitable, as it was still below the maximum recommended current and thus not compromising LED lifetime, while remaining above the point at which the OSL signal began to stabilise.

Table 4: Percent (pct) of maximum input current, input current (I_{input}), and mean operation current (I_{mean}) recorded during stimulation for LED1 and LED2. The mean operational current was also divided by the input current.

LED1	Pct of max I_{input} [%]	11	27	42	58	73	89
	Input current [mA]	10	24	38	52	66	80
	Mean current [mA]	3 ± 5	15 ± 7	29 ± 8	44 ± 8	58 ± 8	72 ± 8
	$I_{\text{mean}}/I_{\text{input}}$	0.3±0.5	0.6 ± 0.3	0.8 ± 0.2	0.8 ± 0.2	0.9 ± 0.1	0.9 ± 0.1
LED2	Pct of max I_{input} [%]	16	30	43	57	70	83
	Input current [mA]	50	90	130	170	210	250
	Mean current [mA]	42 ± 7	82 ± 7	123 ± 7	164 ± 7	204 ± 7	244 ± 7
	$I_{\text{mean}}/I_{\text{input}}$	0.8±0.2	0.91±0.08	0.94±0.05	0.96±0.04	0.97±0.03	0.98±0.03

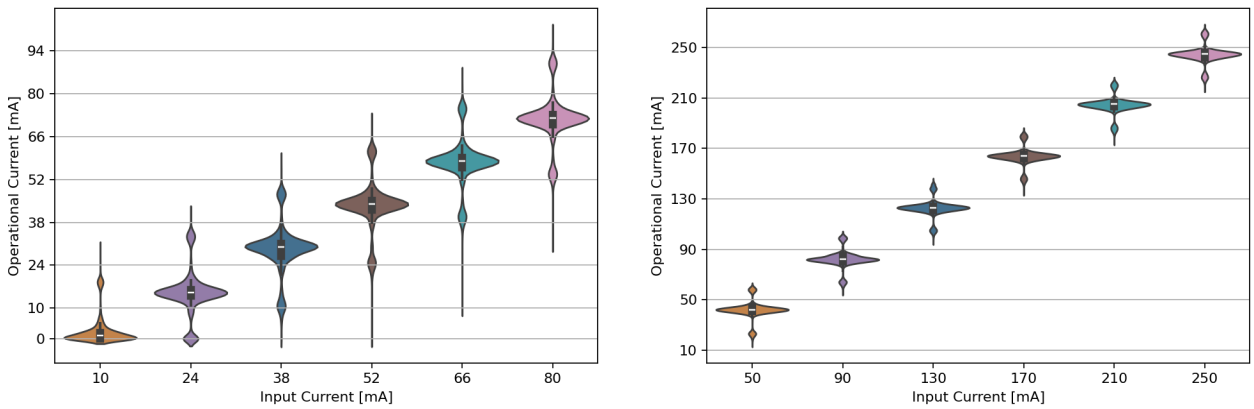

Figure 9: Violin plots of currents recorded every 0.1 s during stimulation using (a) LED1 or (b) LED2, sorted by input current.

4.3 Number of Pellets Per Sample

The signal increased linearly with the number of pellets per sample used for both LEDs, though the trend was stronger for OSL measurements (Fig. 10). When the signal was normalised to mass, it decreased with increasing pellet per sample number. This trend was likely caused by the additional pellets gradually covering a larger portion of the reflective area, which, as shown previously, decreased the signal. Fading may also have played a role in the decrease in signal for samples containing more pellets, considering the required time to complete all measurements.

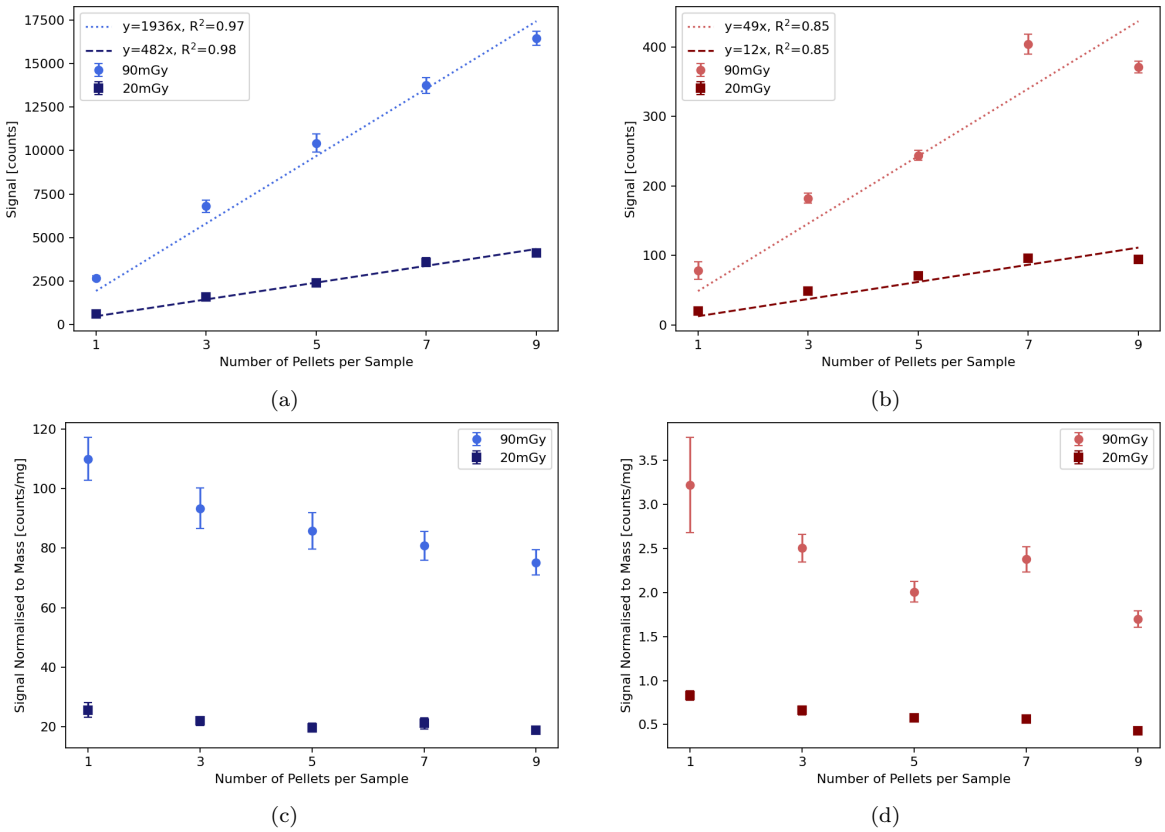

Figure 10: The signal as a function of the number of pellets measured per sample using (a) LED1 or (b) LED2. The signal measured with either (c) LED1 or (d) LED2 was also been normalised to the "mean weight".

The signal normalised to mass was calculated for both "specific weight" as well as "mean weight" for pellets irradiated with 20 mGy, (Fig.11). The signals normalised to mean weight and to specific weight always overlap within their uncertainties; however, the standard deviation was generally smaller when using the specific weight. However, weighing the pellets after each readout was considerably more time-consuming than using a mean value. Overall, for measurements using more than one pellet, if signal normalised to mass is needed, using the mean mass for normalisation seems sufficient. The hope was that the largest signal normalised to mass would be measured when using more than one pellet per sample, since reading more pellets at once would simplify the workflow in an emergency while also providing better statistics. However, since the signal normalised to mass decreased with the number of pellets, using too many pellets per sample is not recommended. Reading out three pellets at once was therefore determined to be the preferred compromise between shortening readout time and improving statistics, while not excessively reducing the signal normalised to mass.

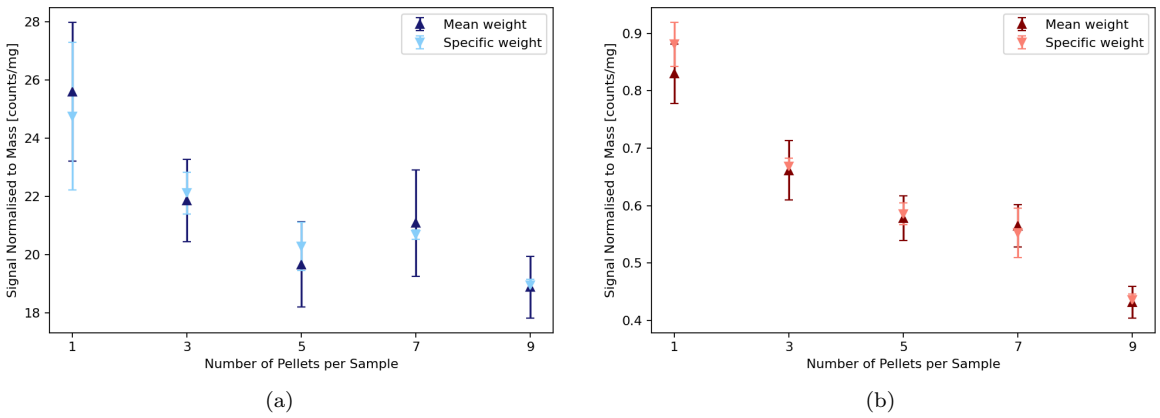

Figure 11: Pellets irradiated with 20 mGy and then normalised to the "specific weight" (mass read out per sample) or "mean weight" (Tab. 1) and then read out using either (a) LED1 or (b) LED2.

4.4 Mass for Measurements of Grains

When readout was performed only 3 h after irradiation, the behaviour of the signal normalised to sample mass was not as anticipated, especially for LED2 (Fig. 12). That is, the normalised signal was expected to increase until the layers of grain grew thick enough that self-absorption of light would occur, whereupon the signal normalised to mass would decrease. Because the expected behaviour was not seen, a systematic error with the method was suspected. It was found that when plotting integrated counts normalised to mass as a function of readout order, an overall decrease in signal as time elapsed was observed (Fig. 12d and Fig. 12c). The readout process was relatively time-consuming, meaning comparisons were made between results read out hours apart without accounting for fading.

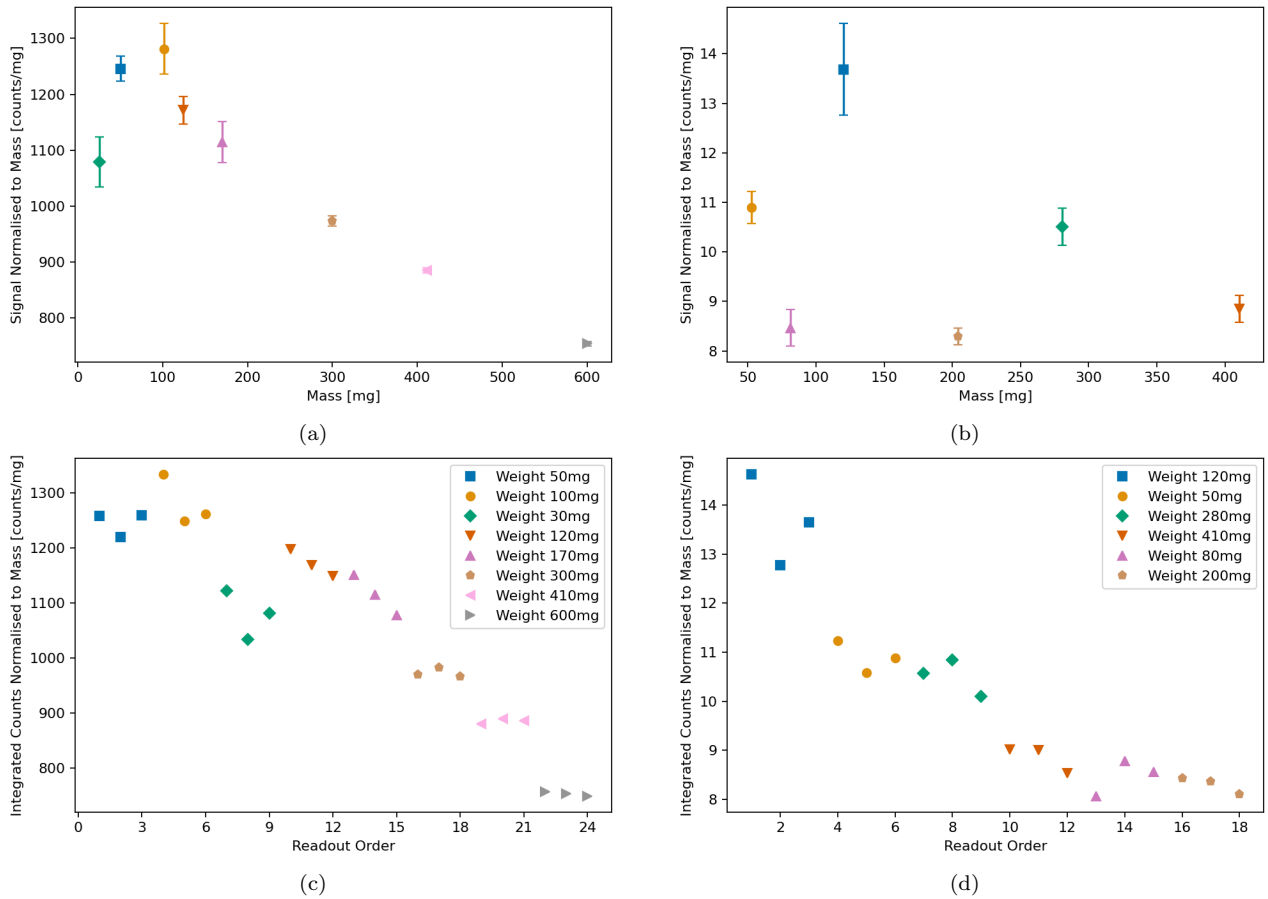

Figure 12: Salt grain samples (Falksalt) of different mass where read out started 3 h after irradiation using (a, c) LED1 or (b, d) LED2, and samples with the same mass (±10 mg) have the same marker. (a, b) The signal normalised to mass has been plotted as a function of sample mass. Integrated (c) OSL counts or (d) IRSL counts normalised to mass for individual readouts has been plotted as a function of readout order.

Because fading was highly suspected to have interfered with the results, the experiment was redone using sachets and a 1 d rest period between irradiation and the start of readout. The relationship between signal and mass was now linear for both LEDs (Fig. 13a and Fig. 13b), and the previously seen trend of integrated counts normalised to mass decreasing as a function of readout order was no longer present (Fig. 13e and Fig. 13f). Note that, due to time constraints, this test was initially performed only for OSL. The signal normalised to mass was highest for samples weighing between 150 mg and 200 mg (Fig. 13c), and the decision to use 150 mg grains per sample for further measurements was made. However, when the experiment was later repeated for IRSL, the normalised signal was highest for samples weighing 200 mg (Fig. 13d). Retroactively, it can thus be concluded that for this salt, using 200 mg per sample would have been a more suitable choice for IRSL. To avoid confusion during an R/N emergency, the same weight would then also be recommended for OSL measurements.

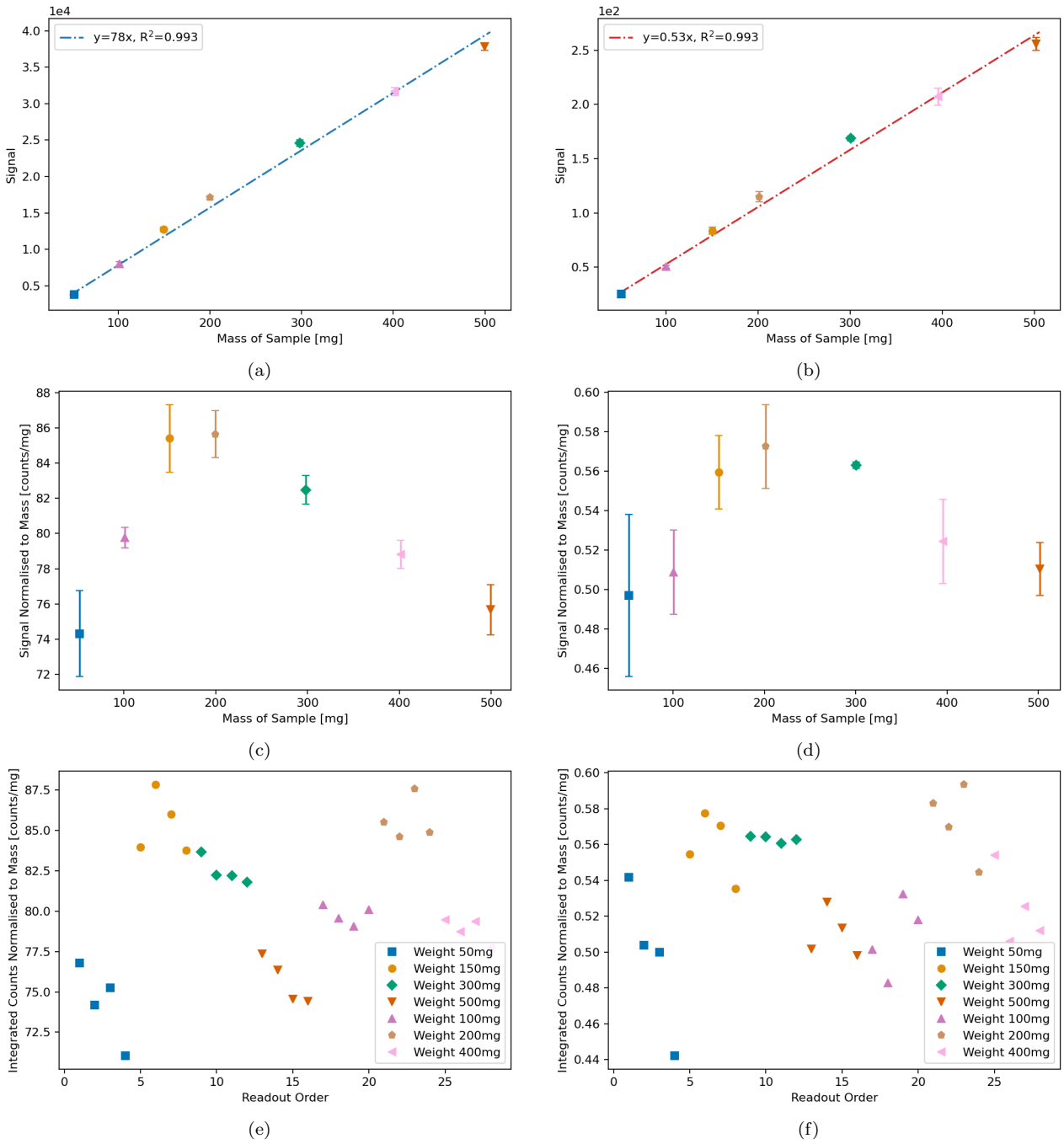

Figure 13: Salt grain samples (sachets) of different mass read out 1 d after irradiation with (a, c, e) LED1 or (b, d, f) LED2, where samples with the same mass (±10 mg) have the same marker. The (a, b) signal or (c, d) signal normalised to mass has been plotted as a function of the sample mass. Additionally, integrated (e) OSL counts or (f) IRSL counts normalised to mass for individual readouts has been plotted as a function of readout order.

4.5 Dose Response and Detection Limits

4.5.1 Pellets

Dose response curves were constructed for the six variations in configurations for the Helios reader, flat or conical holder read out with either LED1, LED2, or LED12 (Fig. 14).

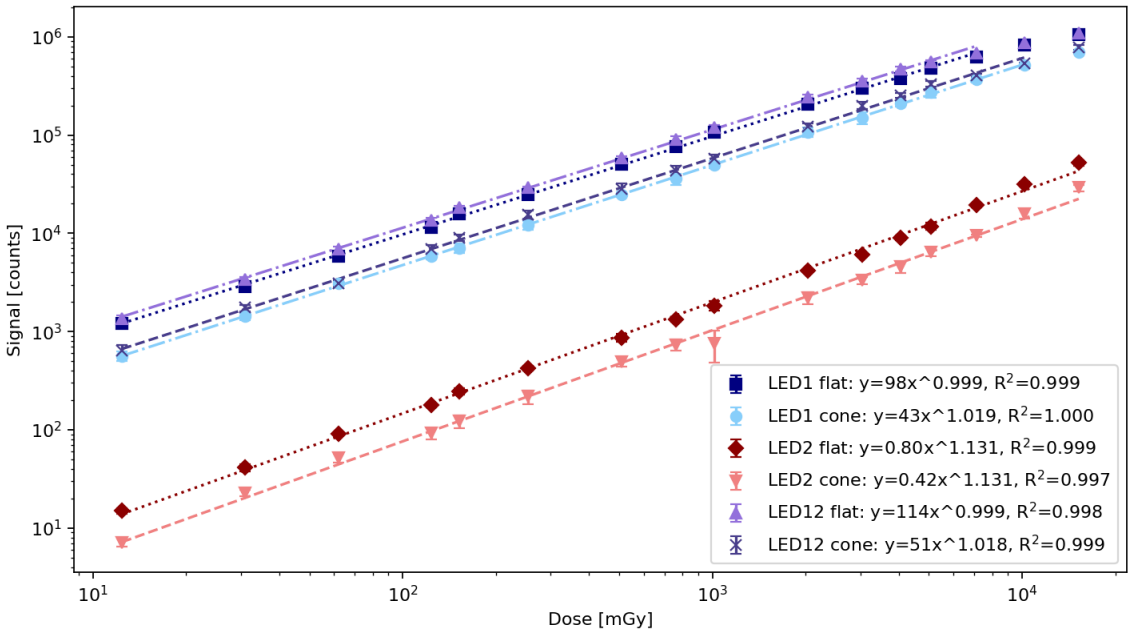

Figure 14: Dose response curves for the Helios reader read out using different configurations (flat or conical holder combined with either LED1, LED2, or LED12) fitted to a power function ($y = ax^b$) using linear regression (least-squares fit). Signal is expressed as a function of the dose received by the samples, displayed in logarithmic scale. Data points where the PMT has been saturated have been included in the figure, but not in the linear regression.

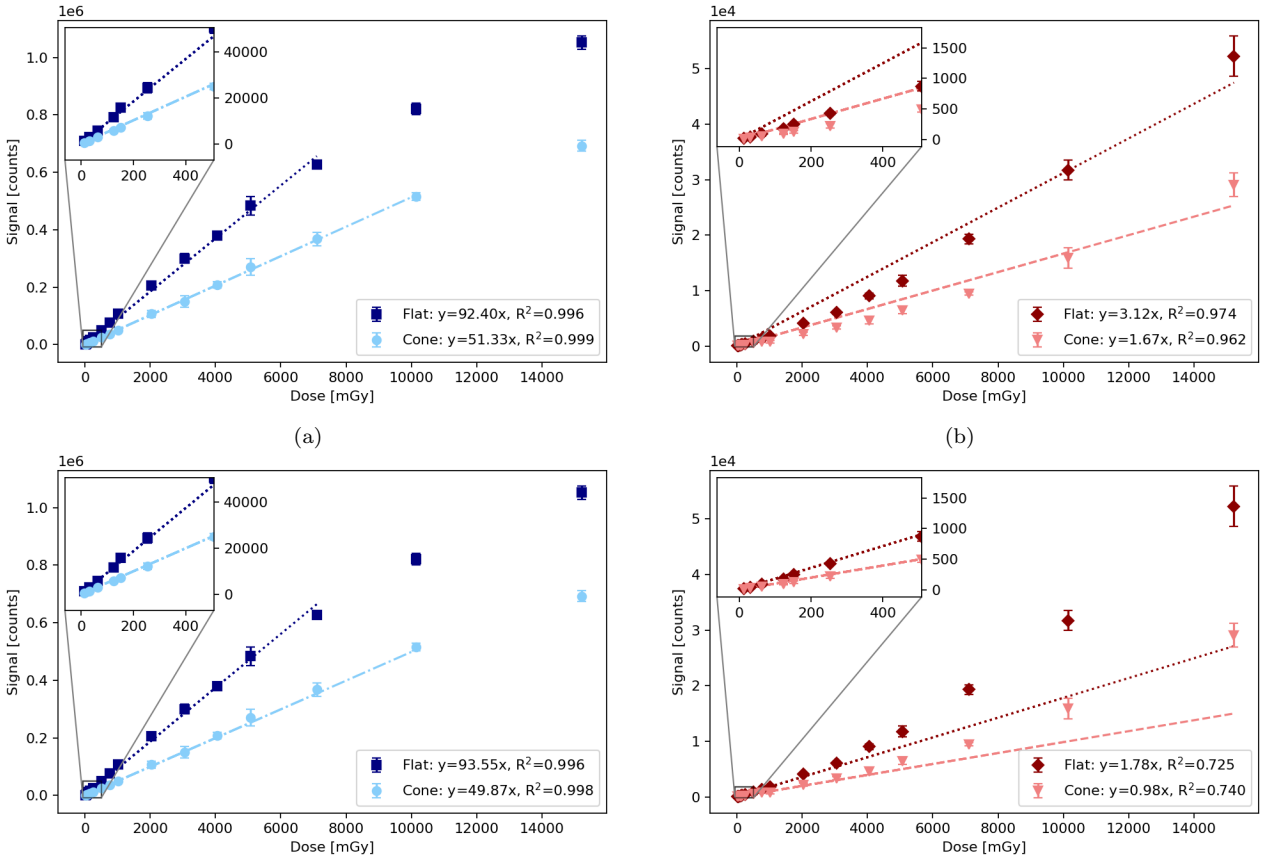

Figure 15: Dose response curves for the Helios reader where samples were read out with either (a, c) OSL or (b, d) IRSL. Signal is expressed as a function of the dose received by the samples, displayed on a linear scale with a zoomed-in section at the lower doses. The linear regression ($y = kx$) has been performed either with (a, b) a least-squares fit or (c, d) a weighted least-squares fit.

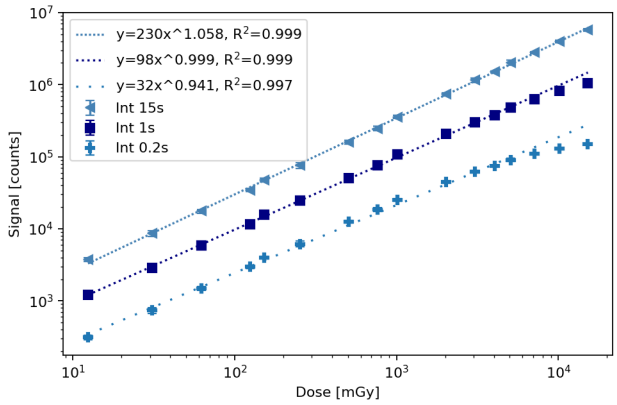

Figure 16: Dose response curve for the flat holder read out with OSL, where the signal has been calculated using three different integration times. Signal is expressed as a function of the dose received by the samples, displayed on a logarithmic scale, and fitted to a power function ($y = ax^b$) using linear regression (least-squares fit). The two data points at 10 Gy and 15 Gy, where the PMT was saturated, were excluded from the fit.

The signal increased linearly as a function of dose for all six configurations measured with the Helios reader (Fig. 14). For LED1 and LED12, the PMT was saturated by 10 Gy for the flat holder and by 15 Gy for the conical holder. The saturation was noticeable at shorter integration times; however, including the remainder of the OSL decay curve "compensated" for it, such that the relationship between dose and signal seemingly remained linear even at doses where saturation occurred (Fig. 16). If there is a future anticipation of receiving doses in the order of multiple Gy, it may be beneficial to include the entire OSL decay curve when constructing a dose response curve.

IRSL displayed supralinear behaviour for both holders, with a b-value of 1.131 (Fig. 14). As a result, there was a noticeable difference depending on whether the weighted least-squares fit was used. When the result was displayed on a linear scale, it became clear that there was an overresponse at high doses when readout was performed with LED2 (Fig. 15b and Fig. 15d). If the resulting k-values are used to reconstruct unknown doses, it is expected that the least-squares fit will produce underestimates at low doses (Fig. 15b) and that the weighted-leats squares fit will produce overestimates at high doses (Fig. 15d). For IRSL to be of use in combination with pellets, it is possible that separate dose response curves for different dose ranges would be needed, which is suboptimal. OSL displayed a very linear behaviour with a b-value very close to 1 (Fig. 14). As a result, there is only a minimal difference between the fits performed with or without a weighted least-squares. As there is a linear behaviour at both high and low doses, it would be preferable to use OSL for dose reconstruction when the samples are pellets.

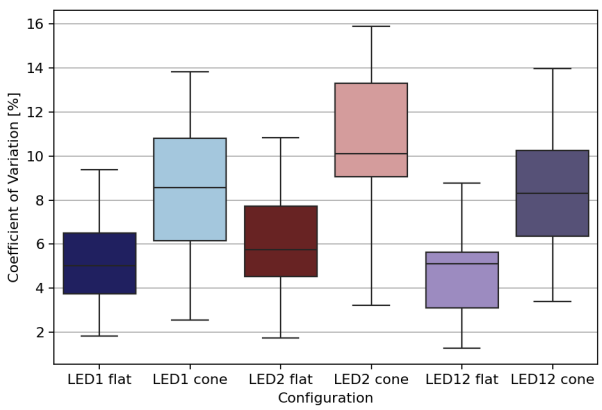

Figure 17: Coefficient of variation (CV) for the six configurations measured with the Helios reader. CV of 36 % for LED2, conical holder, at 1 Gy was excluded from the figure for legibility purposes.

The OSL curves read out using LED1 were smooth at the relatively low dose of 12 mGy (Fig. 31). For IRSL, the curves were more inconsistent at doses below 500 mGy(Fig. 32). Initially, it was speculated that good results would be produced when setting the integration time such that all of the OSL or IRSL curve sans tail was included for samples irradiated with 15 Gy. For OSL, this was deemed to occur around 15 s, and for IRSL, around 30 s. It was later determined that using only the initial part of the decay curve yielded the most reliable results. As previously noted, using only the initial part makes the analysis more vulnerable to saturation; however, when dealing with exposure at doses in the range of daGy, methods other than salt monitoring will likely be used. As in previous tests, the CV was lower for the flat holder compared to the conical (Tab. 3 and Fig. 17).

Similarly to when read out with the Helios reader, the dose response curves read out with the Risø reader displayed a linear increase in signal as a function of dose (Fig. 18), but with an overresponse at higher doses (Fig. 19). Unlike for the Helios reader, this overresponse was visible for both OSL and IRSL.

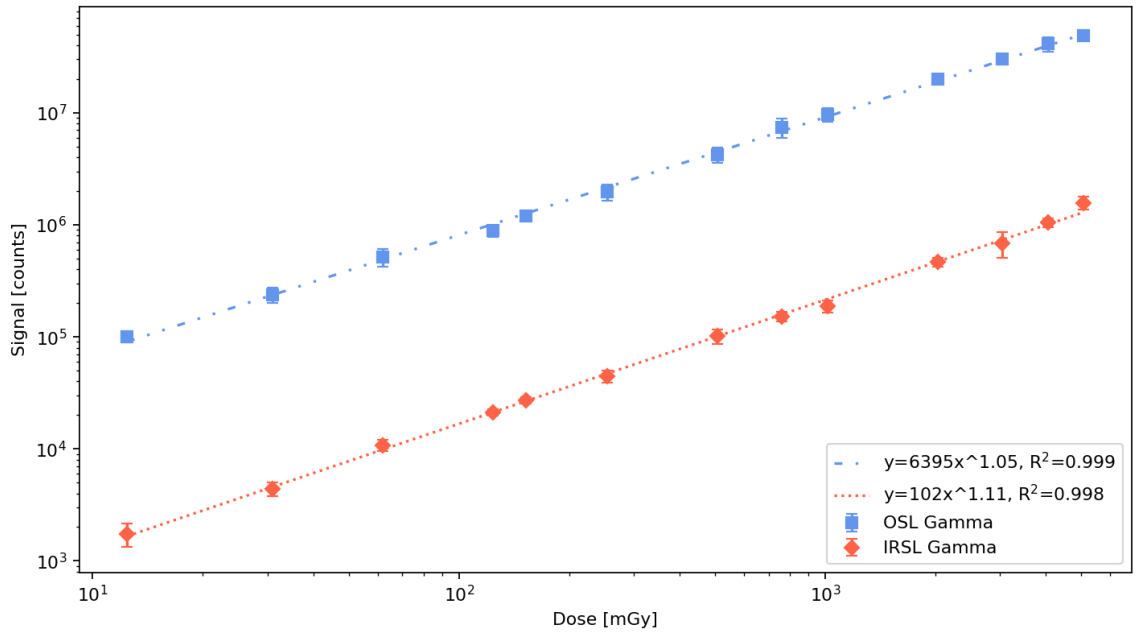

Figure 18: Dose response curves for the Risø reader fitted to a power function ($y = ax^b$) using linear regression (least-squares fit). Signal is expressed as a function of the dose received by the samples, displayed in logarithmic scale.

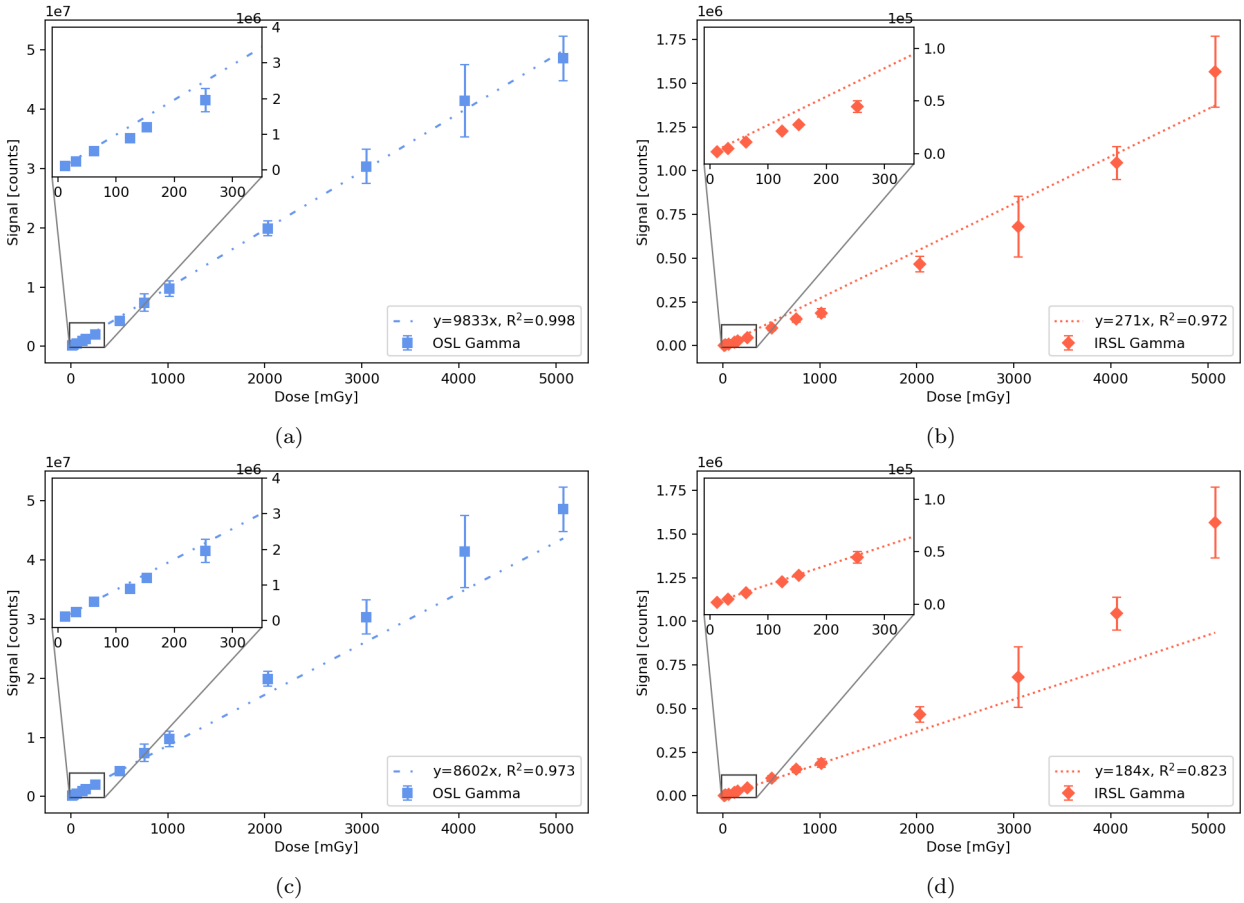

Figure 19: Dose response curves for the Risø reader where samples were read out with either (a, c) OSL or (b, d) IRSL. Signal is expressed as a function of the dose to the samples, displayed on a linear scale with a zoomed-in section at the lower doses. The linear regression ($y = kx$) has been performed either with (a, b) a least-squares fit or (c, d) a weighted least-squares fit.

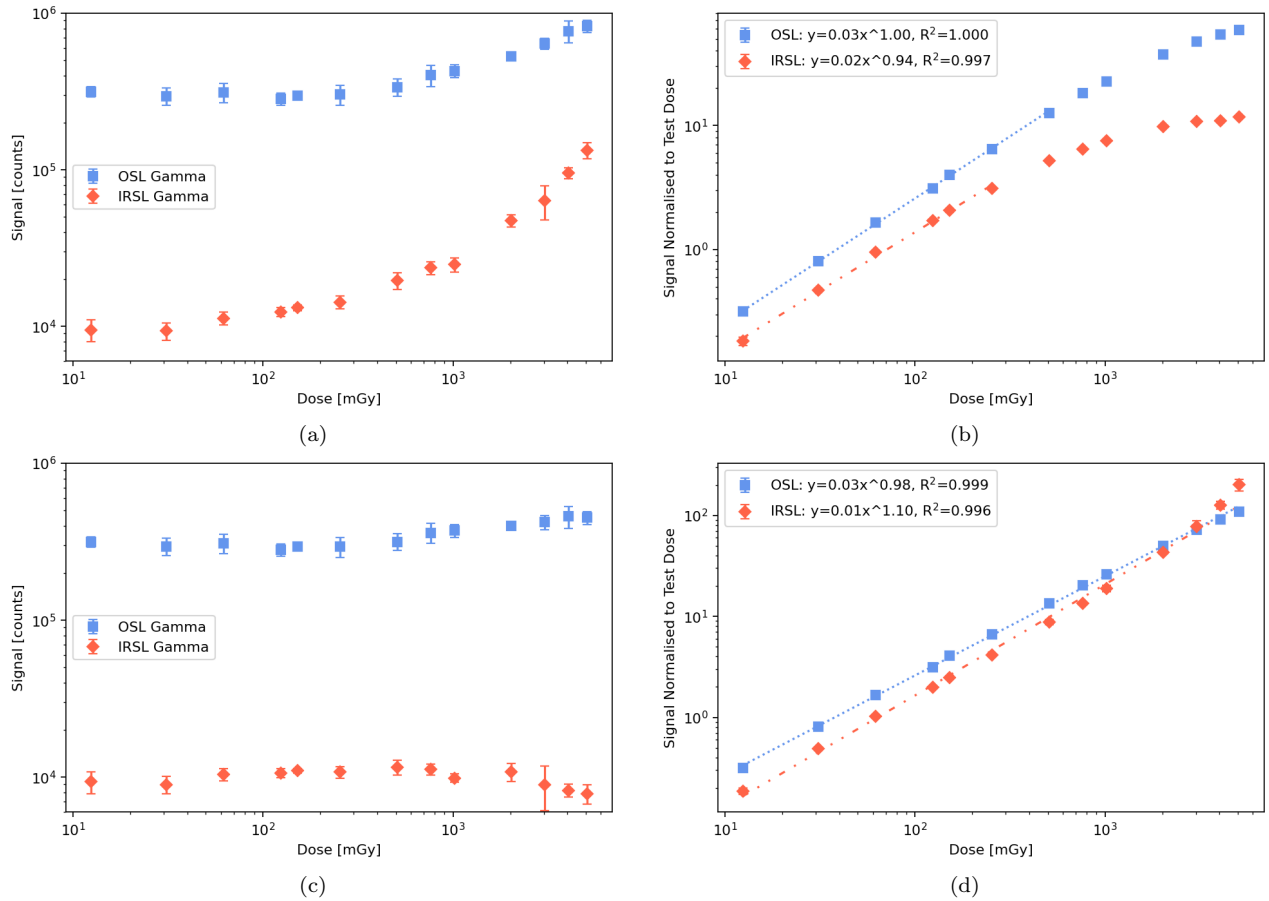

Figure 20: (a) The signal read out after samples had been given a test dose, and (b) the initial readout signal normalised to this test dose. (c) The signal read out after samples had been given a test dose, where the integrated tail-end of the initial readout had been subtracted (Fig. 21), and (d) the initial readout signal normalised to this test dose. All four figures (a, b, c, d) are expressed as a function of the dose the samples received during the initial gamma irradiation at the ^{60}Co source.

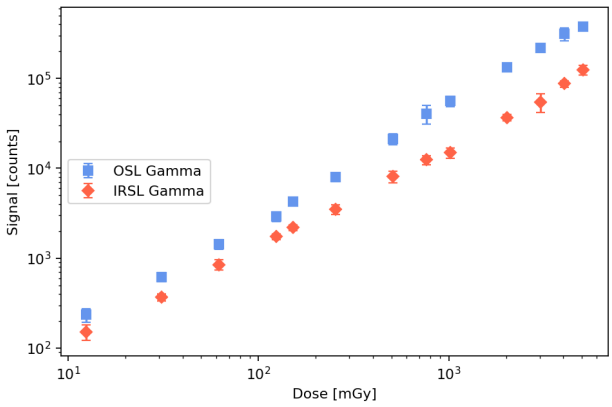

Figure 21: The integrated counts (signal) of the last 1 s of the decay curve tail from the initial readout, where the signal is a result of dose received at the ^{60}Co source.

The samples were given a test dose in the Risø reader. The read out signal was then normalised to the test dose. From the resulting behaviour, it would appear that saturation had occurred (Fig. 20b). However, when studying the signal of the test dose, it was noticed that it increased as a function of the dose given to the samples during the first irradiation, even though one would expect this test dose signal to be constant (Fig. 20a), since the test dose is the same for all samples. The behaviour occurred due to insufficient emptying of the traps during the first readout (Fig. 21). It was thus especially noticeable for IRSL, where traps are never fully depleted. The behaviour could be partly corrected for by integrating the end of the tail from the first readout and subtracting that value from the integrated calibration dose before normalisation (Fig. 20d and Fig. 20c). The behaviour could, for OSL, also have been corrected by using a longer readout time, thereby emptying the traps fully. However, this method is time-consuming and thus not always applicable. Note that for portable readers there is no test dose, which means that insufficient emptying of the traps will not be an issue.

Both MMD and MDD were much lower for the Risø reader than for the Helios reader. However,

the lower readout limits for the Helios reader were still in the order of µGy, and were at least four times lower for OSL compared to IRSL (Tab. 5). Using three pellets per sample and the flat holder allowed measurements of lower doses than with the conical holder. This result further strengthened the notion that measurement using the flat holder and OSL is preferable for the Helios reader. Notably, the MMD for LED12 was slightly lower than for LED1, but not to a degree that was considered meaningful. In an R/N emergency, it would still be preferable to use OSL, which has been thoroughly studied, than the combination of blue and IR light, of which less is known.

Table 5: MMD and MDD for the Helios and Risø readers. For the Helios reader, six different configurations were investigated for gamma-irradiated pellets (two different holders and three variations of light sources), and for the Risø reader, gamma-irradiated pellets were read out with either OSL or IRSL.

			OSL/LED1	**IRSL/LED2**	**LED12**
MMD [µGy]	**Helios**	Cone	400 ± 100	3000 ± 1300	340 ± 80
		Flat	210 ± 50	1500 ± 500	190 ± 40
	Risø		1.5 ± 0.9	30 ± 30	-
MDD [µGy]	**Helios**	Cone	130 ± 30	800 ± 400	100 ± 20
		Flat	60 ± 20	400 ± 200	60 ± 10
	Risø		0.4 ± 0.3	10 ± 10	-

4.5.2 Grains

The dose response curves for grains showed a near linear behaviour between the signal and the dose received by the samples (Fig. 22). However, supralinear behaviour was once again observed, with an overresponse at high doses. Further, OSL showed a larger overresponse than IRSL.

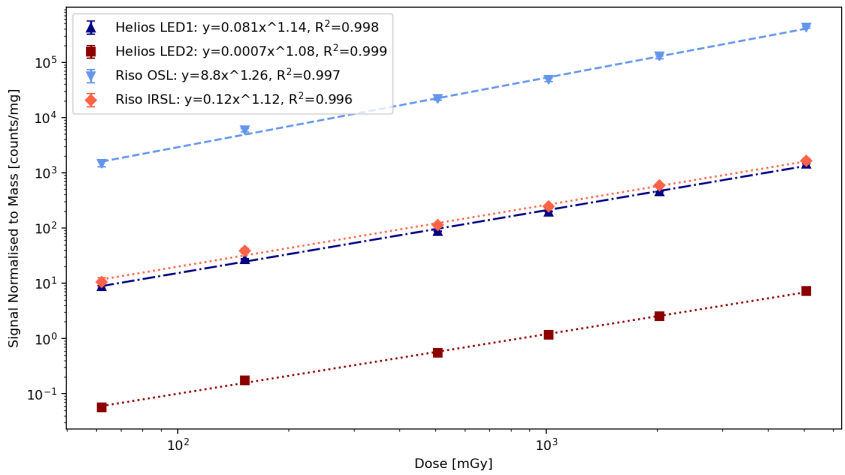

Figure 22: Dose response curves for the Helios and Risø readers fitted to a power function ($y = ax^b$) using linear regression (least-squares fit). Signal is expressed as a function of the dose received by the samples.

The MMD and MDD were much lower for the Risø reader than the Helios reader (Tab. 6). For OSL, the MMD was in the order of µGy, allowing it to be used in epidemiological studies where such doses are expected. For IRSL, the MMD was in the order of mGy and had a large standard deviation, which is not optimal for epidemiological studies, but still useful for triaging purposes, especially since the overresponse at high doses was less than for OSL. Note that the optimal mass 200 mg was not used during these readouts, but rather 150 mg. Changing the mass may alter the results.

The OSL curves obtained with LED1 were, as for the pellets, smooth at a relatively low dose (Fig. 33a), while the curves were more inconsistent at lower doses for IRSL, which contributed to the relatively large MDD (Fig. 33b). The original plan was to set the integration time such that all of the OSL or IRSL curve sans tail was included in the integration for samples irradiated with

5 Gy which for both OSL and IRSL was deemed to be around 10 s. Like for pellets, it was determined that a shorter integration time was preferable.

Grains would be highly useful during an R/N emergency, but primarily using IRSL and not at low doses. However, for the dose response curve to be fully applicable, it should be constructed with more doses than the six that were used in this work.

Table 6: MMD and MDD for the Helios and Risø readers, with samples read out either with OSL or IRSL.

		OSL/LED1	**IRSL/LED2**
MMD [µGy mg^{-1}]	**Helios**	500 ± 200	$20\,000 \pm 10\,000$
	Risø	9 ± 5	800 ± 1100
MDD [µGy mg^{-1}]	**Helios**	160 ± 40	5000 ± 3000
	Risø	3 ± 1	200 ± 300

4.6 Dose Recovery Test

For samples exposed to lower doses, the reconstructed dose often differed from the theoretical dose (Fig. 23). This behaviour was observed due to the overresponse at high doses in the dose response curves (least-squares fit), which were used to obtain the sensitivity utilised during the dose reconstruction. To illustrate with an example, in Fig. 19a (Risø, OSL, pellets, integration time 1 s), data points and/or the standard deviation lay below the fitted line, noticeably so at low doses. As such, while 3462 mGy was within the uncertainty of the reconstructed dose using that sensitivity (Fig. 23a), for 197.8 mGy the reconstructed dose was an underestimation (Fig. 23c).

The reconstructed dose most closely matching the theoretically calculated dose was obtained with the Helios reader for pellets read out with OSL, integrated over 1 s (Fig. 23). It had a delta percentage (percentage change) under 10 % for all three blind tests (Tab. 7). The consistent result occurs because the linear regression was the most reliable across the dose range.

For pellets read out with IRSL, fading is likely to have affected the results. To illustrate, the dose response curve (Fig. 15b) predicted that the reconstructed dose for exposure at 3462 mGy should be an underestimation of the theoretical dose, which was not observed (Fig. 23a). The dose response curve was constructed using measurements taken two days after irradiation. In contrast, the dose reconstruction measurements were performed 1 day after irradiation, resulting in a higher signal because less fading had occurred. Should IRSL be used during R/N emergencies, waiting for the signal to stabilise is crucial for dose response and reconstruction.

Table 7: Reconstructed doses (D_R) that have a delta percentage ($\Delta\%$) within 30 % of the theoretical dose (D_T). The delta percentage is included in the table. For the setup, samples in which grains have been used are shortened to G., while P. corresponds to pellets. It is noted whether samples were read out with OSL or IRSL, and how many seconds of the resulting OSL/IRSL decay curve were integrated when signal and sensitivity were calculated.

D_T		3462 mGy		1484 mGy		197.8 mGy	
	Setup	D_R [mGy]	$\Delta\%$ [%]	D_R [mGy]	$\Delta\%$ [%]	D_R [mGy]	$\Delta\%$ [%]
Helios	IRSL G. 10 s	3383	-2.3	1272	-14	149	-25
	IRSL G. 1 s	3487	0.72	1321	-11	155	-21
	OSL P. 1 s	3136	-9.4	1389	-6.4	181	-8.6
	IRSL P. 30 s	3869	12	1384	-6.7	155	-21
	IRSL P. 1 s	4433	28	1626	9.6	193	-2.6
Risø	IRSL G. 1 s	311	-10	1197	-94	143	-27
	IRSL P. 1 s	4468	29	1477	-0.47	187	-5.5

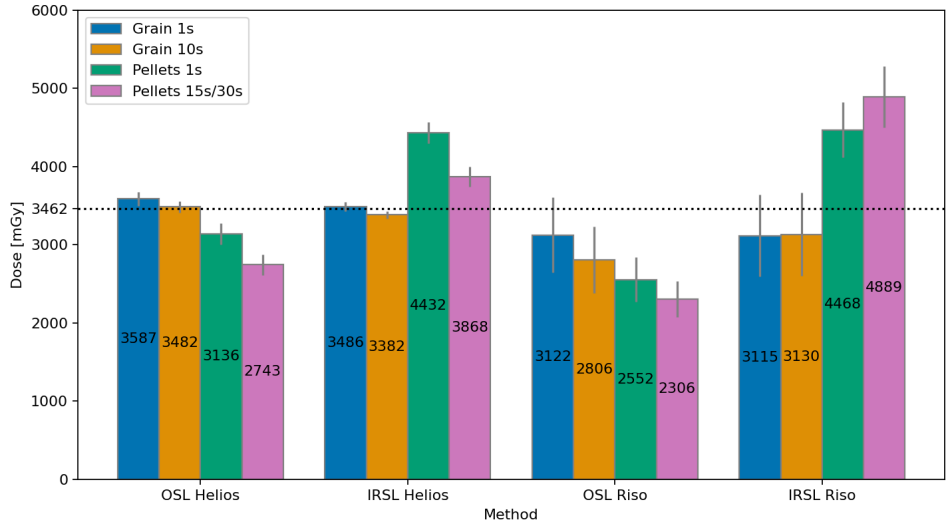

(a)

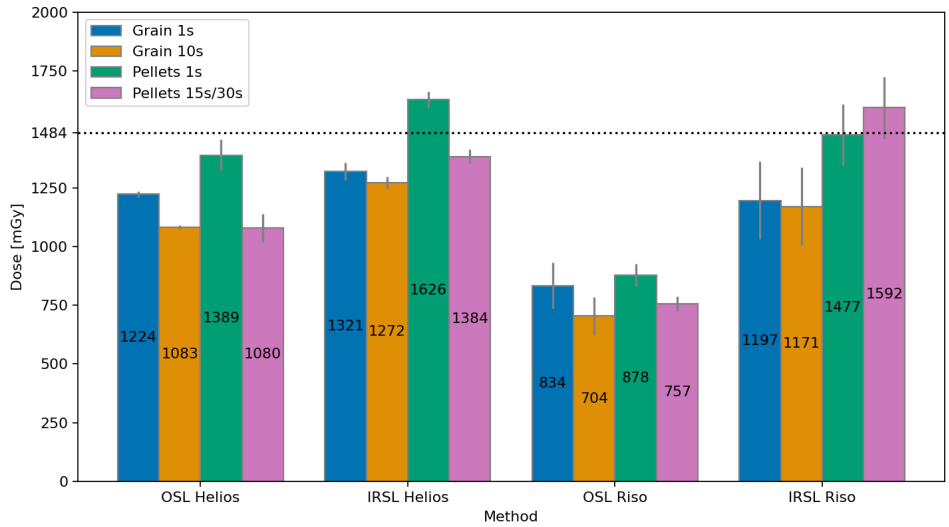

(b)

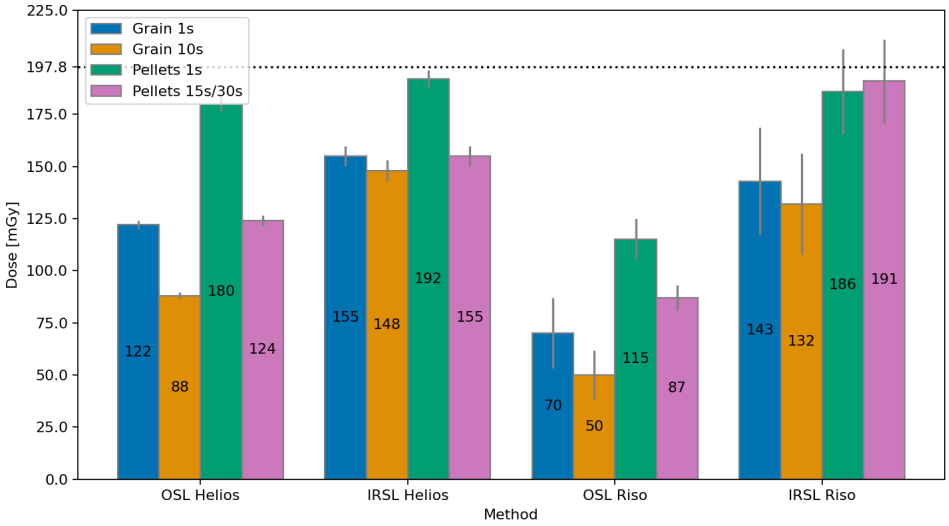

(c)

Figure 23: Doses reconstructed from readouts with the Helios or the Risø reader, using OSL or IRSL, expressed as bars. The decay curves were integrated over either 1 s for all setups, 10 s for grains, 15 s for pellets read out with OSL, or 30 s for pellets read out with IRSL. The reconstructed dose obtained with each method is displayed in the middle of the corresponding bar, and the standard deviation is shown as a line through the top of the bar. The theoretical doses are (a) 3462 mGy, (b) 1484 mGy, and (c) 197.8 mGy. The theoretical dose is expressed as a dotted line across the corresponding figure.

In an R/N emergency, an uncertainty of 30 % between the reconstructed and theoretical dose is allowed. The reconstructed doses in Fig. 23 that satisfy this requirement are displayed in Tab. 7. While the most consistently correct reconstructed dose was obtained with OSL (pellets, integration time 1 s), all other reconstructed doses included in the Tab. 7 were read out with IRSL.

4.7 Fading

4.7.1 Pellets

For readouts with IRSL, comparably rapid fading was observed during the first hours following irradiation, after which the signal began to stabilise and remained as such for at least 50 d (Fig. 24). Thus, readouts conducted with IRSL after a rest of at least 1 d, but preferably more, do not need to be corrected for fading, provided the sensitivity was also measured after the initial rapid fading had passed. Readouts conducted in the Risø reader with OSL instead displayed a rapid increase in signal, so-called inverse fading, in the hours after irradiation. By the next day, the signal began to stabilise, and it reached a stable state by the two-week mark after irradiation. For readout with OSL using the Helios reader, an initial decrease in signal occurred during the first hours following irradiation, until 1 d had passed, at which point inverse fading was observed. The increase in signal persisted for at least a month after initial irradiation, after which a trend towards stabilisation seems to occur (Fig. 24d). Correction for fading may be necessary should pellets be read out with OSL in the Helios reader weeks after initial irradiation. For pellets, the signal never went above double nor below half of its initial value within a month of initial irradiation (Fig. 25).

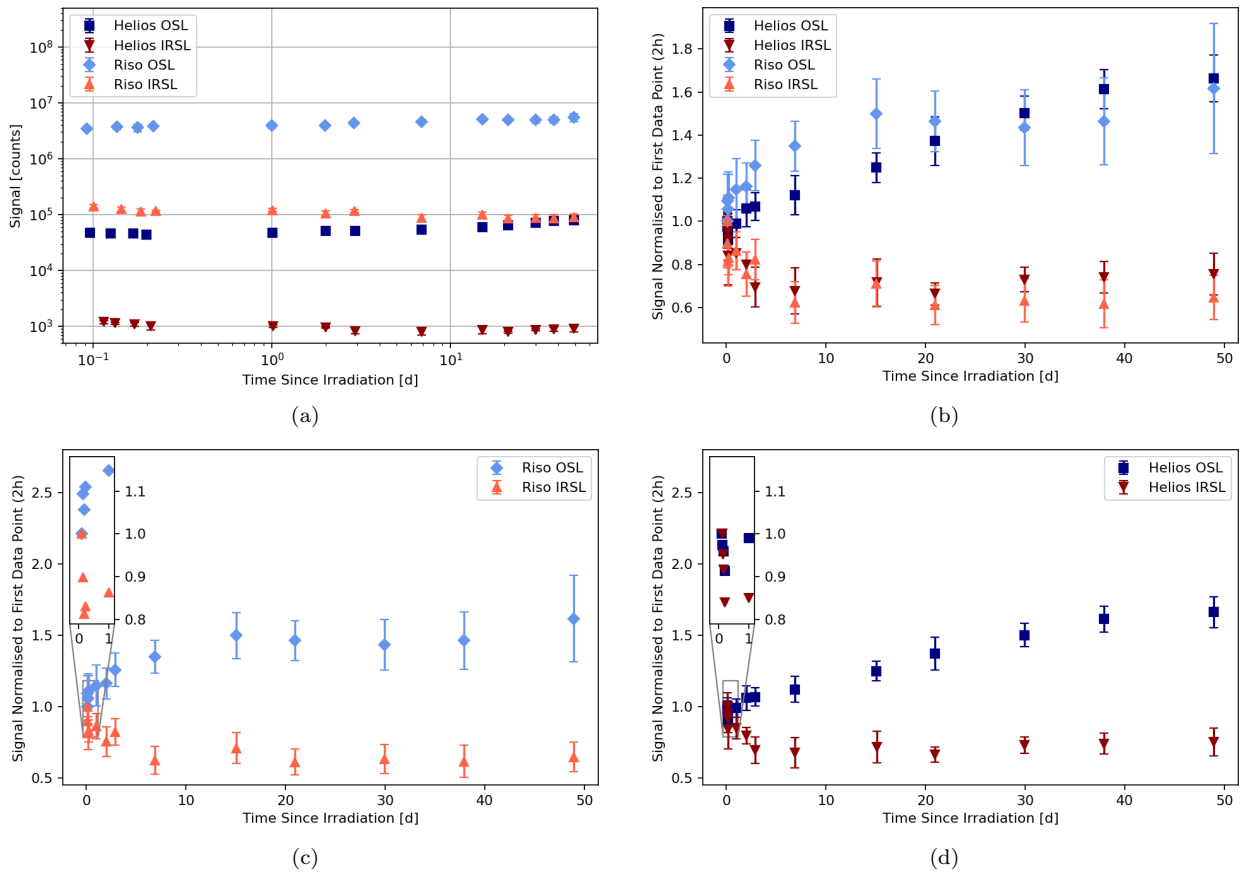

Figure 24: (a) The signal of pellets irradiated with 500 mGy and read out with OSL or IRSL in the Helios or the Risø reader, plotted as a function of time between irradiation and readout in log-scale. The signal normalised to the first data point as a function of time elapsed since readout on a linear scale for (b) all four variations, (c) readouts conducted with the Risø reader, or (d) readouts conducted with the Helios reader. The inset plots in (c, d) show a zoomed-in section of readouts conducted up to the first day after irradiation, with error bars excluded for visibility purposes.

4.7.2 Grains

For grain samples read out with the Helios reader, fading the first hours after irradiation had already been observed in earlier tests (Fig. 12c and Fig. 12d). After this, inverse fading was observed for at least 15 d after irradiation for OSL (Fig. 25d), with a rate of signal increase which appeared similar to the one observed for the pellets also read out with OSL (Fig. 24d). However, for IRSL, inverse fading was observed for grains up to one week after irradiation, unlike for the pellets, but it stabilised after this point for at least 15 d(Fig. 25d). Thus, correcting for fading is needed for OSL. For IRSL, correcting is not needed given that both measurements during R/N emergencies and for dose response curve creation are made after a one-week rest period. When the grains were read out in the Risø reader, there was a relatively large standard deviation in signal, likely due to the allowance of mass deviation up to 25 % of 20 mg (Fig. 25c). Despite this, the signal did appear stable for both OSL and IRSL for at least 15 d after irradiation. The fading behaviour varied between pellet and grain samples, due in part to different components in the salt (the pellets contained iodine, while the grains in the sachets did not), and in part to the size of the grains themselves (the sieved grains used to make pellets were smaller than grains from the sachets). The fact that the grains in the pellets were mechanically pressed together might also have altered the crystal structure, which, in turn, could have affected the material's behaviour.

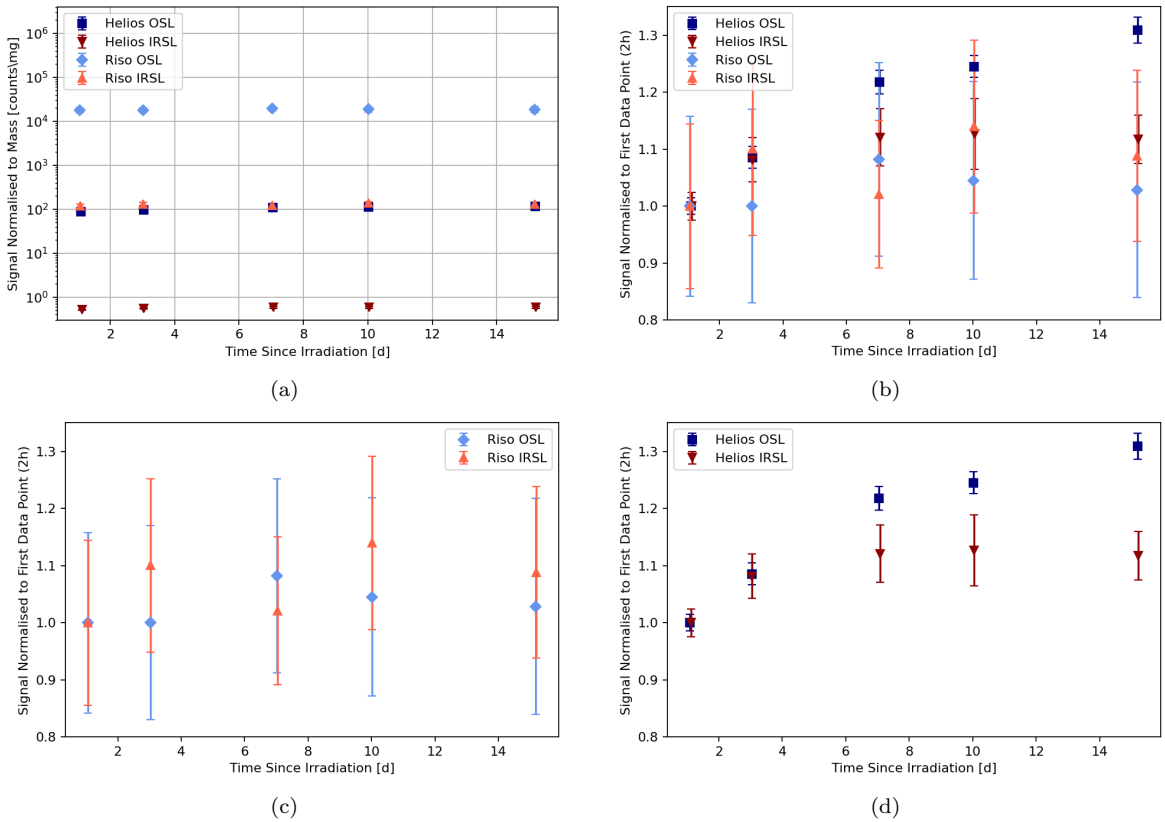

Figure 25: (a) The signal normalised to sample mass of grains irradiated with 500 mGy and read out with OSL or IRSL in the Helios or the Risø reader, plotted as a function of time between irradiation and readout in log-scale. The signal normalised to the first data point as a function of time elapsed since irradiation in linear scale for (b) all four variations, (c) readouts conducted with the Risø reader, or (d) readouts conducted with the Helios reader.

4.8 Pellet Orientation During Irradiation and Readout

There was a difference in the distribution of integrated counts depending on whether the side of the pellet being read out coincided with the side facing the source during irradiation, except for gamma irradiated pellets read out with IRSL (Fig. 26). Because the integrated counts for each configuration were not normally distributed, a Mann-Whitney U-test was performed to determine whether the difference in integrated counts was significant. The alpha value was set to 5 % ($\alpha = 0.05$). The

difference was significant for beta irradiated pellets and gamma irradiated pellets read out with OSL (Tab. 8). The question remained whether the significant difference would affect measurements during R/N emergencies. The delta percentage between the mean integrated counts for each configuration was for OSL 12 % and 11 %. For triage during an R/N emergency, that difference would not be overly problematic. Yet, for research where a more exact dose may be required, the significant difference in integrated counts depending on pellet orientation at readout could prove to be problematic and thus needs to be investigated further.

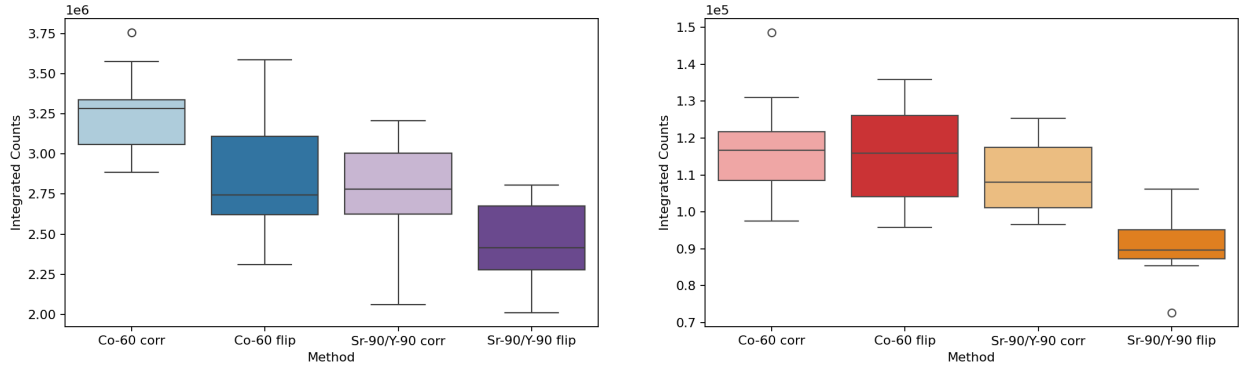

(a) (b)

Figure 26: Pellets, irradiated with either gamma (Co-60) or beta (Sr-90/Y-90), were read out with the side which faced the source during irradiation placed up (corr) or down (flip) in the sample holder. Samples was read out out with either (a) OSL or (b) IRSL.

For beta-irradiated pellets, the difference in integrated counts may have occurred due to the beta-particle penetration depth in salt, as more energy was likely deposited on the side facing the source. However, for gamma-irradiated pellets, energy was expected to be deposited evenly throughout the samples due to the greater penetration depth. That this behaviour occurred only for gamma-irradiated pellets read out by IRSL, but not by OSL, thus necessitates further study.

Table 8: The p-values from a Mann-Whitney U-test with the null hypothesis that there is no significant difference between the signal from pellets read out with the side which faced the source during irradiation placed up, and the signal from pellets that had been flipped before readout. The delta percentage (Δ%) is also included. Samples were either read out with OSL or IRSL and irradiated with gamma (Co-60) or beta (Sr-90/Y-90).

	OSL		IRSL	
Irr. Source	Co-60	Sr-90/Y-90	Co-60	Sr-90/Y-90
p-value	0.045	0.038	0.85	0.0017
Δ% [%]	-12	-11	-1.5	-17

4.9 Accidental Light Exposure

There was a variation between the integrated counts for salt samples exposed to red light for different time durations (Fig. 27). A one-way Kruskal-Wallis H-test ($\alpha = 0.05$) was performed to test the null-hypothesis that there was no significant difference in means between the groups of samples left out in red light for different amounts of time. The result indicated a significant difference for pellets, while the null hypotheses was not rejected for grains (Tab. 9). However, the integrated OSL counts normalised to a test dose in Fig. 27c and Fig. 27d decreased as a function of the time they were exposed to red light. As the figures implied, there was a significant difference between the means of the integrated OSL counts normalised to a calibration dose (Tab. 9). This behaviour suggests that red light in the standard laboratory environment, to some extent, affected the traps of the samples. Further research is therefore needed to investigate this phenomenon.

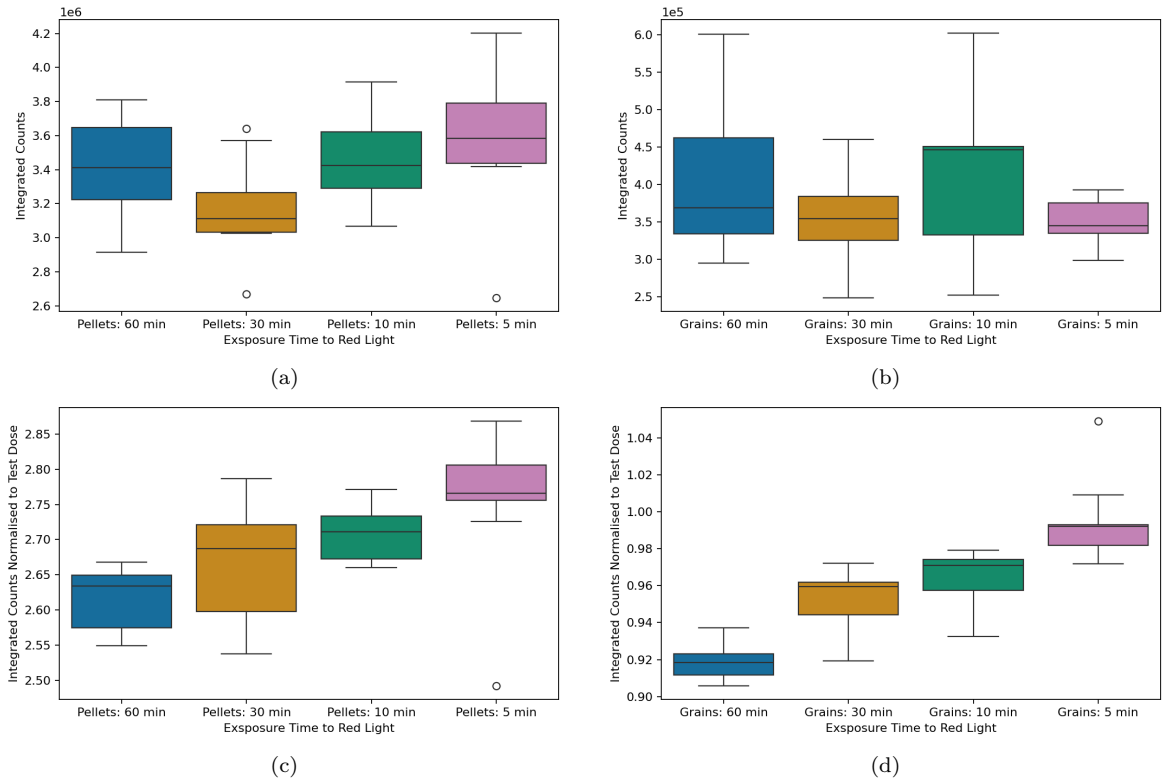

Figure 27: (a, c) Pellets or (b, d) grains placed in the Risø reader sample carousel under red light for either 60, 30, 10, or 5 min, and then read out by OSL. (a, b) The integrated counts of the OSL curves or the (c, d) the integrated counts of the OSL curves normalised to a calibration dose.

Table 9: The p-values from a one-way Kruskal-Wallis H-test with the null-hypothesis that the difference in means between the groups displayed in Fig. 27a, Fig. 27b, Fig. 27c, and Fig. 27d was not significant. For $p < \alpha = 0.05$ the null hypothesis was discarded, indicating significant difference.

	p-value	
	Not Normalised	Normalised
Pellets	0.046	1.0×10^{-3}
Grains	0.42	4.9×10^{-6}

Samples were exposed to one of three different light sources: a computer screen, a phone screen, or a lamp. The integrated OSL counts were noticeably lower for samples exposed to lamp light (Fig. 28). When a one-way Kruskal-Wallis H-test was performed on the four groups in Fig. 28, the mean difference proved significant (p-values 6×10^{-15} for pellets and 2×10^{-8} for grains). A Mann-Whitney U-test, with the null hypothesis that there was no significant difference between pellets exposed only to red light and those exposed to both red light and an additional light source, was used to further investigate the groups in Fig. 28. According to the Mann-Whitney U p-values, only for samples exposed to the regular room lamp was there a significant difference, both for pellets and grains (Tab. 10). In the remaining accidental light-exposure scenarios, the null hypothesis was not rejected. However, although the test did not indicate a significant difference for pellets exposed to light from a phone screen, the p-value of 0.063 was close to the alpha value. In other words, it was nearing statistical significance, suggesting a trend might become visible with a larger sample size. So, while it follows that a flash of light from an electronic screen might not ruin an OSL measurement of salt samples by emptying all traps, minimising or, preferably, entirely avoiding additional light sources is preferable.

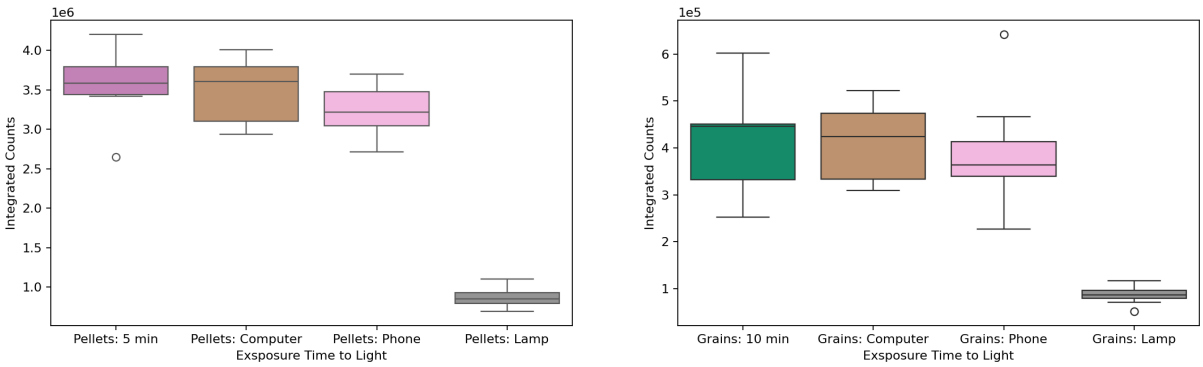

(a) (b)

Figure 28: Samples exposed to computer, phone, or lamp-light for 5 min and then placed in the Risø reader sample carousel while exposed to red light for (a) 5 min for pellets or (b) 10 min for grains. The samples were compared with pellets or grains exposed to only red light for the same duration required to prepare the samples.

Table 10: The p-values from a Mann-Whitney U-test with the null-hypothesis that there was no significant difference between the integrated counts of samples, (a) pellets or (b) grains, exposed to nothing but red light and those exposed to an additional light source. The addition light source was either a computer screen, a phone screen, or a lamp.

	p-value		
Light Source	Computer	Phone	Lamp
Pellets	0.79	0.063	4.1×10^{-4}
Grains	0.93	0.53	4.1×10^{-4}

4.10 Limitations

The manual switch between samples in the Helios reader restricted how quickly samples could be measured, allowing only a limited number of tests to be run in a single day. On average the readout speed was 3 min per measurement, such that one dose response curve for 10 mGy-15 Gy took between 3 h and 4 h to complete. As a result, limited sample sizes were used. In future research, repeated measurements on different days would increase the sample size. Further, larger sample sizes would be beneficial for testing environmental effects, making trends more visible.

A rest period of at least 1 d between irradiation and readout should be enforced to minimise fading effects. However, for measurements that may take multiple hours or days to finish, a longer rest period might be employed to allow the signal to fully stabilise before starting. Otherwise, fading corrections could prove beneficial for both OSL and IRSL.

The lack of a unirradiated control samples stored with the irradiated samples introduced an additional uncertainty due to dose contributions from the natural background, albeit a minor one. A contribution of size µGy was not considered large enough to affect results for measurements where the samples were stored for up to 2 d between irradiation and readout. For longer storage periods, such as for fading, the natural background contribution was larger, but still considerably smaller than the dose of 500 mGy. However, should tests be conducted with samples exposed to lower doses, further research using control samples could become relevant.

Another limitation was that samples irradiated at the ^{60}Co source were transported between Lund and Malmö and thus exposed to environmental factors, such as different temperatures, which may have affected the results. If, and in such a case, by how much this would have impacted the stored signal would need to be further investigated.

5 Conclusion

Both NaCl in the form of grains and pellets show potential for dose monitoring when read out with the portable reader Helios. For pellets, OSL is superior when it comes to both dose reconstruction and ability to measure low doses, which are points of interest during R/N emergencies, especially for epidemiological studies. The method's main disadvantage is the persistent inverse fading, but this may be corrected for. For grains, IRSL is more promising than OSL for dose reconstruction and it does not require fading corrections when longer storage periods are applied. Although there is a limitation due to the high MDD for grains read out with IRSL, grains would primarily be used during triage, where high doses are of interest, which makes this a minor issue.

Further research may be needed to determine optimal readout geometry, as initial measurements were made under the impression that waiting one hour between irradiation and the start of readout was sufficient to avoid fading. But this is only true for readouts that run almost simultaneously. For Helios, where each readout is carried out individually and thus more time consuming, fading influences the result on this timescale. Other points necessitating further investigation is environmental factors. Due to time limitations, this study did not investigate the effect of the humidity and temperature on the luminescence signal, but such study may be beneficial for the purpose of the applications. In addition, the effect of the accidental light exposure on the calibration dose signal should be investigated.

To reiterate, a network of portable readers in combination with NaCl appears feasible for dosimetric applications during R/N emergencies. However, further investigation is required.

Acknowledgments

First, I would like to express my gratefulness to my supervisors, Maria Karampiperi, for your invaluable counselling, steady support, and ceaseless willingness to offer aid throughout this entire process; and Christian Bernhardsson, for always offering advice when needed and being a well of ideas that drove the project forward. I would also like to offer thanks to Mikael Westin for your assistance with laboratory work and kind words of encouragements, as well as to everyone else at the Department of Radiation Physics, Skåne University Hospital (SUS), Malmö for the warm welcome and inclusion in the community.

Second, I would like to thank the people at the Oncology Clinic Radiotherapy, SUS, Lund, for helping arrange irradiation sessions at the ^{60}Co source, and a special word of gratitude to Benedek Hunor for your assistance with calibrating the dose rates. Thanks also to 3D Centrum, SUS, Malmö, for printing the lightproof holders utilised during multiple measurements in this work.

Finally, I want to extend my appreciation to the incredible support network that is my friends and family, I lack the words to describe just how much you mean to me.

References

[1] A Axelsson, P Kock, J Johansson, J Lindgren, AM Blixt Buhr, J Boson, U Bäverstam, and S Karlsson. Radiological consequences of fallout from nuclear explosions (2023:05e). Swedish Radiation Safety Authority (SSM), 2023.

[2] International Atomic Energy Agency (IAEA). International framework. Available: `http://www.iaea.org/topics/international-framework`, n.d. [accessed 2026-03-02].

[3] International Atomic Energy Agency. *Generic Procedures for Medical Response During a Nuclear or Radiological Emergency.* EPR-MEDICAL. IAEA, 2024. ISSN 2518-685X.

[4] M Karampiperi, CL Rääf, and C Bernhardsson. Evaluation of a portable osl/irsl reader for radiation dose assessment of nacl pellets–in situ individualised screening during r/n emergencies. *Radiation Measurements*, 179:107323, 2024.

[5] V Chumak, E Bakhanova, M Karampiperi, and C Bernhardsson. Osl dosimetry with table salt for mass screening of individual doses during radiological or nuclear emergencies. *Radiation Measurements*, 177:107233, 2024.

[6] C Bernhardsson, CL Rääf, and S Mattsson. Spatial variability of the dose rate from 137cs fallout in settlements in russia and belarus more than two decades after the chernobyl accident. *Journal of environmental radioactivity*, 149:144–149, 2015.

[7] M Christiansson, T Geber-Bergstrand, C Bernhardsson, S Mattsson, and CL Rääf. Retrospective dosimetry using salted snacks and nuts: a feasibility study. *Radiation Protection Dosimetry*, 174(1):1–5, 2017.

[8] DTU Physics, Department of Physics, Risø, Denmark. *Guide to The Risø TL/OSL Reader*, 2021.

[9] E Yukihara and SWS McKeever. *Optically stimulated luminescence: fundamentals and applications.* John Wiley & Sons, 2011.

[10] L Waldner. *Optically stimulated luminescence dosimetry with NaCl pellets. Dosimetry for prospective applications.* Phd thesis, Lund University, 2021.

[11] KJ Thomsen. *Optically stimulated luminescence techniques in retrospective dosimetry using single grains of quartz extracted from unheated materials.* Phd thesis, Risø National Laboratory, 2004.

[12] IK Bailiff, S Sholom, and SWS McKeever. Retrospective and emergency dosimetry in response to radiological incidents and nuclear mass-casualty events: a review. *Radiation Measurements*, 94:83–139, 2016.

[13] JF Barquinero, P Fattibene, V Chumak, T Ohba, S Della Monaca, C Nuccetelli, K Akahane, O Kurihara, K Kamiya, A Kumagai, et al. Lessons from past radiation accidents: Critical review of methods addressed to individual dose assessment of potentially exposed people and integration with medical assessment. *Environment international*, 146:106175, 2021.

[14] M Christiansson, C Bernhardsson, T Geber-Bergstrand, S Mattsson, and CL Rääf. Osl in nacl vs. tl in lif for absorbed dose measurements and radiation quality assessment in the photon energy range 20 kev to 1.3 mev. *Radiation Measurements*, 112:11–15, 2018.

[15] L Waldner, CL Rääf, Y Hinrichsen, L Herrnsdorf, and C Bernhardsson. Experimentally determined and monte carlo–calculated energy dependence of nacl pellets read by optically stimulated luminescence for photon beams in the energy range 30 kev to 1.25 mev. *Journal of Radiological Protection*, 40(4):1321–1335, 2020.

[16] L Waldner and C Bernhardsson. Physical and dosimetric properties of nacl pellets made in-house for the use in prospective optically stimulated luminescence dosimetry applications. *Radiation measurements*, 119:52–57, 2018.

[17] P Morthekai, M Jain, AS Murray, KJ Thomsen, and L Bøtter-Jensen. Fading characteristics of martian analogue materials and the applicability of a correction procedure. *Radiation Measurements*, 43(2-6):672–678, 2008.

[18] Salinity AB Falksalt. Finkornigt salt med jod. Available: `https://falksalt.se/produkter/finkornigt-salt-med-jod/`, n.d. [accessed 2026-05-05].

[19] L Waldner, CL Rääf, and C Bernhardsson. Nacl pellets for prospective dosimetry using optically stimulated luminescence: Signal integrity and long-term versus short-term exposure. *Radiation and environmental biophysics*, 59(4):693–702, 2020.

[20] Nordana A/S. Salt i portionspak: Breve - 1 g. x 2000 stk - multi-text. Available: `https://www.nordana-as.dk/produkter/kolonial/salt-i-brev-1-g-x-2000-stk-multi-text/`, n.d. [accessed 2026-05-06].

[21] ZERO-RAD, Czestochowa, Poland. *Helios User Manual*, 2025.

[22] ET Enterprises Ltd, Uxbridge, United Kingdom and Sweetwater, USA. *photodetector module PDM TTL series data sheet*, 2017.

[23] DTU Nutech, Center for Nuclear Technologies, Risø, Denmark. *Risø TL/OSL Sequence Editor*, 2016.

[24] G Upton and I Cook. *A dictionary of statistics 3e*. Oxford University Press, 2014.

[25] JL Devore. *Probability and Statistics for Engineering and the Sciences 8e*. CENGAGE Learning, 2011.

[26] R Chen and SWS McKeever. *Theory of thermoluminescence and related phenomena*. World Scientific, 1997.

A Appendix

A.1 Lightproof Holders

In the case of an R/N emergency in which salt pellets are to be used for monitoring, a lightproof holder is needed to prevent any stable traps from being emptied. Such potential holders had already been developed by the Department of Medical Radiation Physics, and printed by 3D Centrum, SUS, Malmö. However, the holders' ability to stop light from penetrating had yet to be verified through trial; thus, a lightproof test was conducted. 50 pellets were irradiated with a dose of 45 mGy in Risø, whereupon they were transferred to ten 3D-printed holders, five pellets in each holder, as shown in Fig. 29. Half of the holders were placed in a mylar bag, which was in turn placed in a cupboard, treated in dark conditions. These holders have been denoted "shielded". The remainder of the holders were stored in an environment with a mix of direct sunlight and artificial light, denoted "unshielded". After 3 h readout began in Risø (20 s), whereafter a test dose of 45 mGy was given and read out 1 h later.

Figure 29: To the left, positioning of five pellets in an open 3D-printed holder with capacity up to nine pellets. To the right, an example of what the 3D printed holder looks like when closed.

The signals normalised to the test dose did not appear to differ depending on whether the holders with the samples were stored in darkness or in light, both for individual samples and for the mean of all samples kept in the same holder (Fig. 30). When performing a Mann-Whitney U-test with the null hypothesis that there was no significant difference between the normalised signals as a function of storage conditions, with $\alpha = 0.05$, the resulting p-values were 0.8 for samples plotted individually and 1.0 for the mean of samples stored in the same holder, meaning that there was no indication of a significant difference. The holders were deemed lightproof.

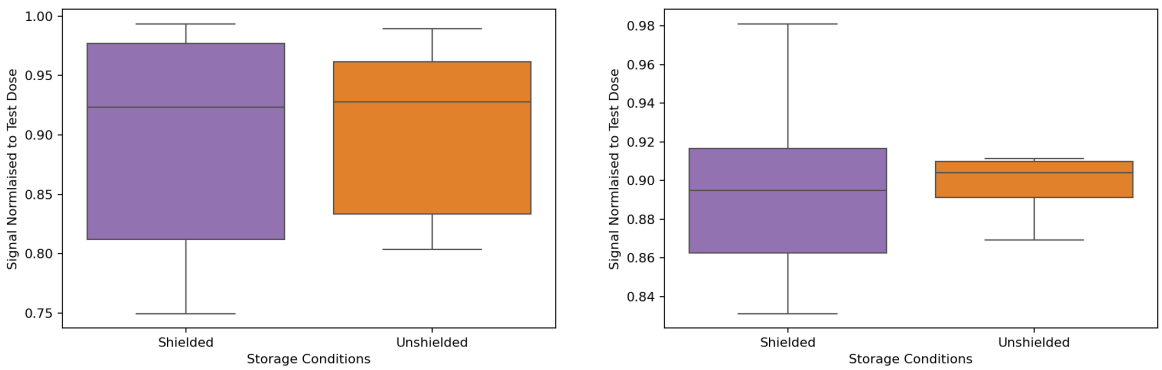

(a) (b)

Figure 30: Signal normalised to a test dose for (a) all samples or (b) the mean of samples stored in the same holder, divided into groups depending on whether the holders were stored in darkness (shielded) or in direct sunlight (unshielded).

A.2 Dose Response (OSL/IRSL Decay Curves)

The doses samples received after irradiation during the dose response test are in Tab. 11. The OSL and IRSL decay curves for both pellets and grains read out with Helios are in Fig. 31, Fig. 32 and Fig. 33.

Table 11: The doses samples were irradiated with during the dose response test, rounded to two significant figures.

Reader(s) **Samples** **Type of radiation**	**Dose** [mGy]
Helios & Risø Pellets Gamma, ^{60}Co	12, 31, 62, 120, 150, 250, 510, 760, 1000, 2000, 3000, 4100, 5100, 7100*, 10000*, 15000*
Helios & Risø Grains Gamma, ^{60}Co	62, 150, 510, 1000, 2000, 5100

* Only read out with Helios

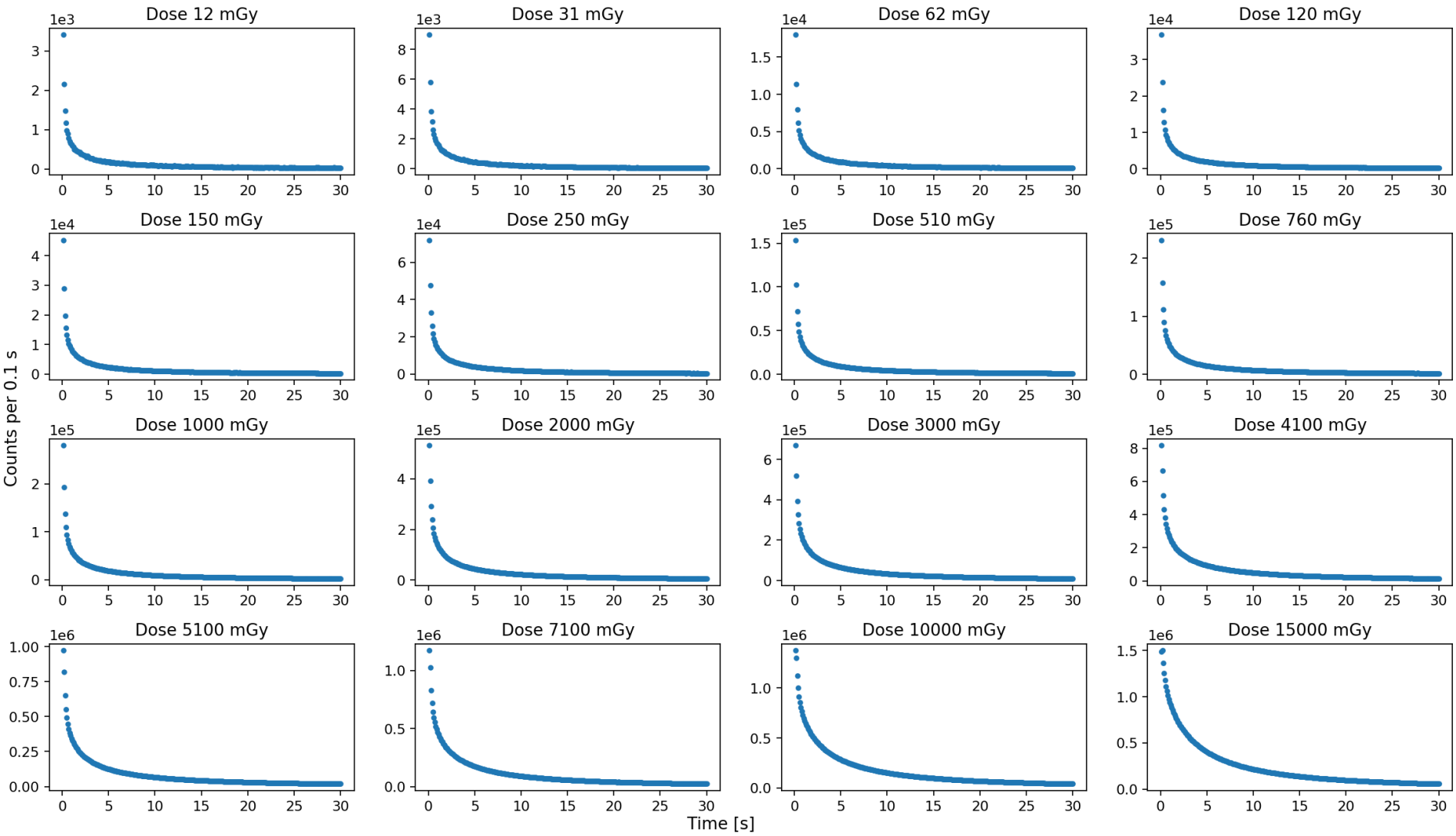

Figure 31: OSL decay curve for samples irradiated with 16 different doses and read out with the Helios reader using LED1 and the flat sample holder. OSL counts per 0.1 s are displayed as a function of readout time.

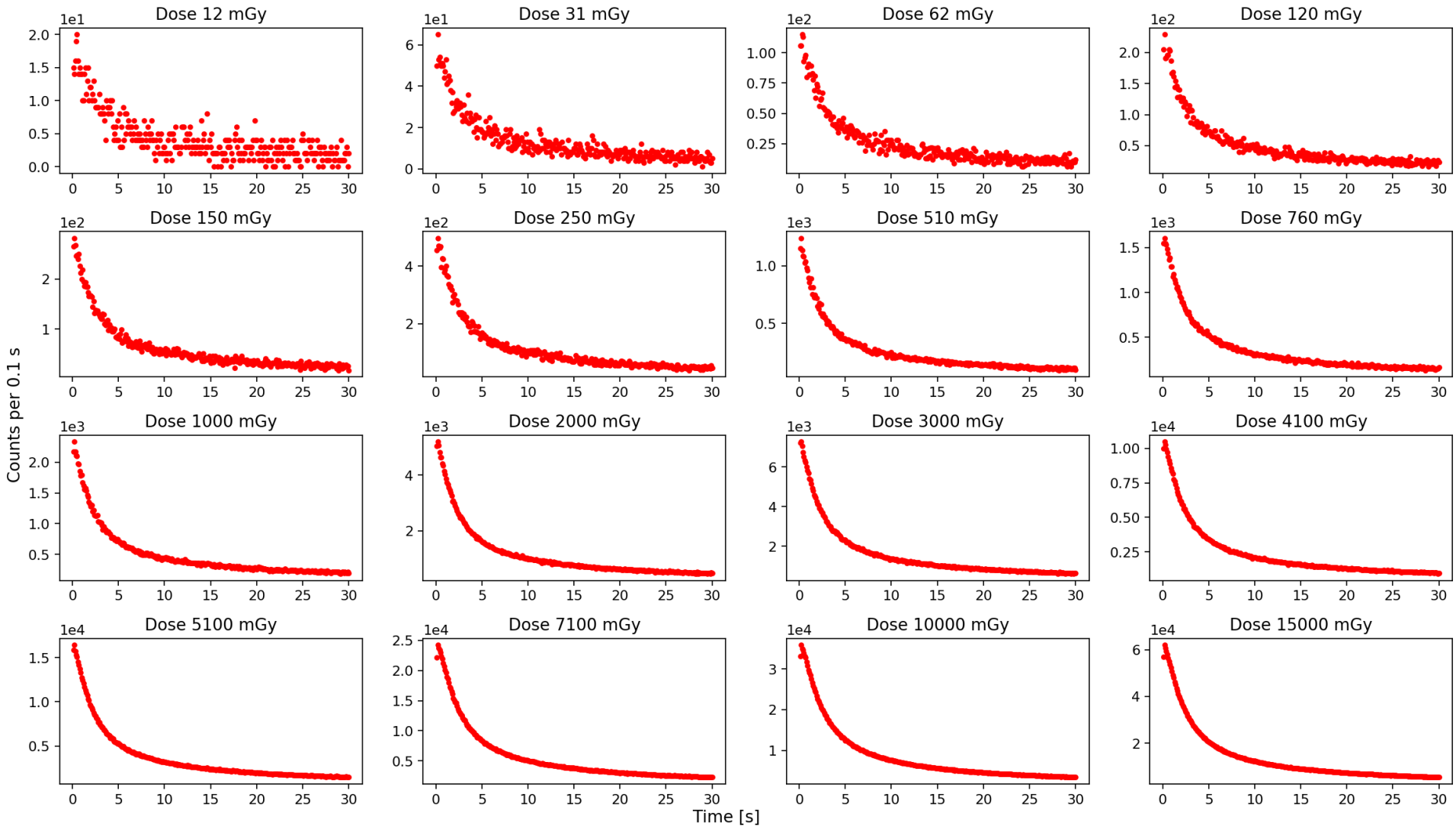

Figure 32: IRSL decay curve for samples irradiated with 16 different doses and read out with the Helios reader using LED2 and the flat sample holder. IRSL counts per 0.1 s are displayed as a function of readout time.

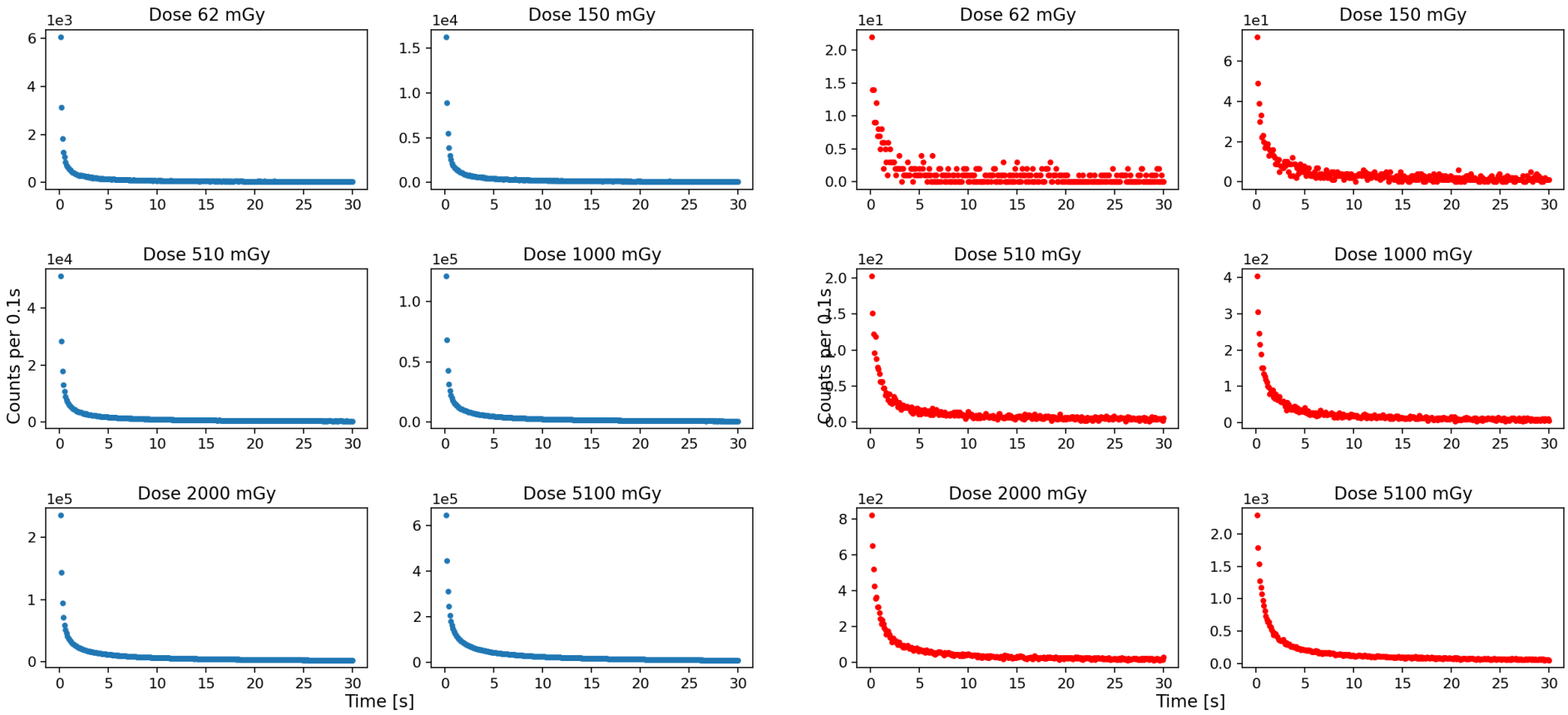

Figure 33: (a) OSL and (b) IRSL decay curve for samples irradiated with six different doses and read out with the Helios reader. Counts per 0.1 s are displayed as a function of readout time.